

Wire-based Gaseous Detector Technologies

Peter Wintz (FZ Jülich, Germany)

Contact: p.wintz@fz-juelich.de, pwintz@cern.ch

.. and inputs from DRD1 collaborating groups

Outline - Wire-based Detectors

1. Introduction

1. Overview
2. 56' years developments

2. Detector basics

1. Ionization and drift
2. Amplification and operation modes
3. Signal readout
4. Drift gases
5. Wire aspects and ageing

3. Measurements and resolutions

1. Drift time and spatial resolution
2. Momentum resolution
3. Particle identification methods

4. Detectors and applications

1. Systems in experiments
2. Layouts and specifications
3. Highlights
4. Range of applications

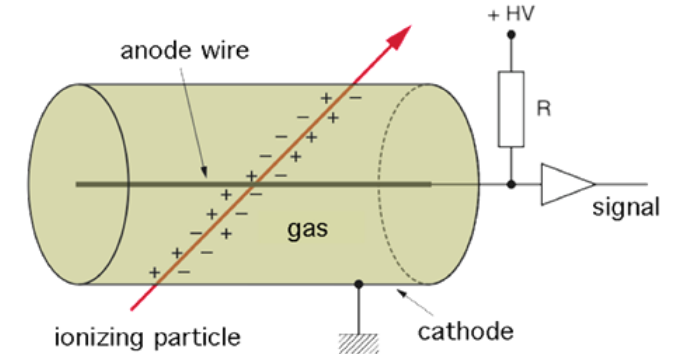
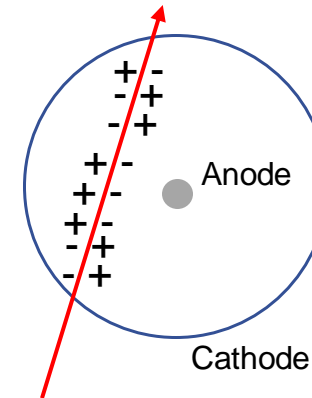
5. Summary

6. Research projects in DRD1

1.1 Overview

- **Wire chamber** (simplest geometry example)

- anode wire on the axis of a gas-filled cylinder
- metallized cylinder surface is the cathode
- charged particle track ionizes the gas atoms or molecules
- electric field between anode and cathode separates e- and pos. ions
- number of electron-ion pairs is proportional to the particle energy-loss (dE/dx)
- electrons drift to the anode, arrival time gives space information

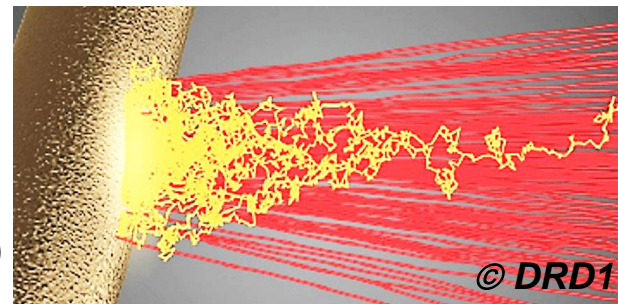
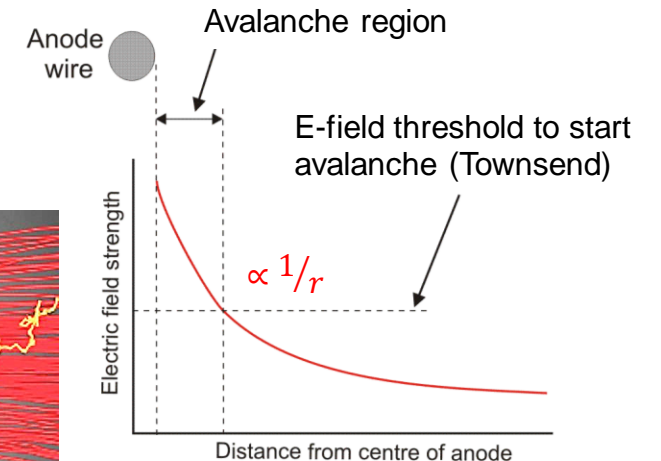


$$E(r) = \frac{1}{r} \frac{V}{\ln(b/a)}$$

r ... distance from the wire
 a ... radius of anode wire
 b ... radius of cathode cylinder

- **Signal**

- by choosing very thin wires ($\varnothing \sim 20\text{-}30\mu\text{m}$) strongly increasing E-field close to the wire
- then strong e- acceleration and secondary gas ionizations by Coulomb collisions with gas atoms
- avalanche of ionizations with charge multiplication (factor A)
- localized avalanche per incoming e- in proportional mode ($A \sim 10^3\text{-}10^5$)
- drift of electrons and slower ions induce a signal on the wire



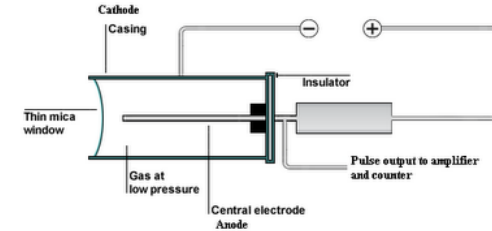
Avalanche simulation (Garfield) of *electrons* and *positive ions*.

© DRD1

1.2 History

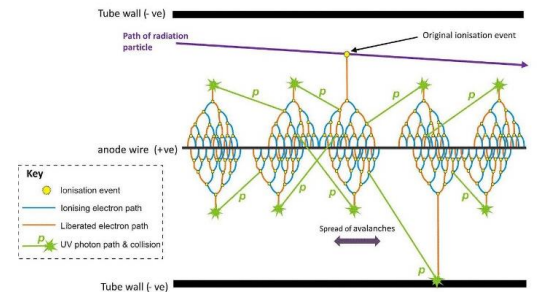
• Geiger Counter (1908*)

- counter for α -particles, led to Rutherford's nuclear theory of the atom (Nobel Prize 1908)
- operation voltage such that sufficient amplification for signal, but that gas discharge terminates
- gas discharge ($A \sim 10^8 - 10^{10}$) by UV-photons produced during avalanche
- UV-photons further ionize gas and make photo-effect at cathode: means no localized particle information
- only radiation detection, e.g. radiation counter as dose meter



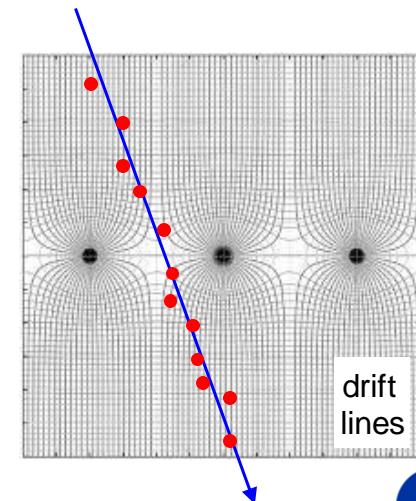
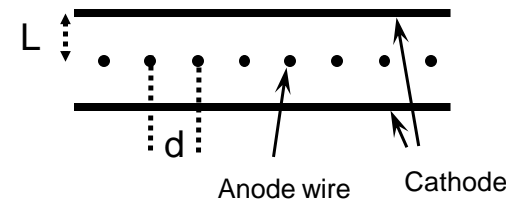
[Http://miniphysics.blogspot.com](http://miniphysics.blogspot.com)

Spread of avalanches in a Geiger-Müller tube



• Multi wire proportional chamber (1968*)

- the first position sensitive gas detector
- chamber with multiple anode wires, each working as a proportional counter
- wires with distance d to neighbors gives space point : $\sigma_x \approx \frac{d}{\sqrt{12}}$ (e.g. $\sigma_x \approx 577\mu\text{m}$, $d = 2\text{mm}$)
- MWPC invented by Charpak et al. at CERN in 1968, Nobel prize in 1992

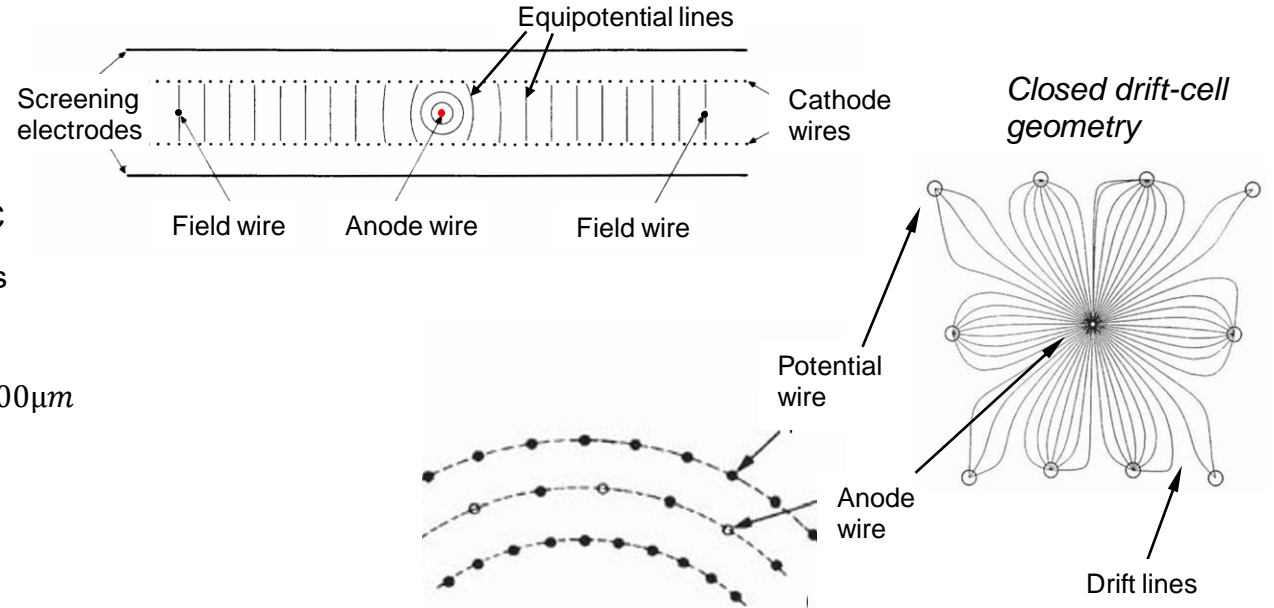


*Year of invention

1.2 History

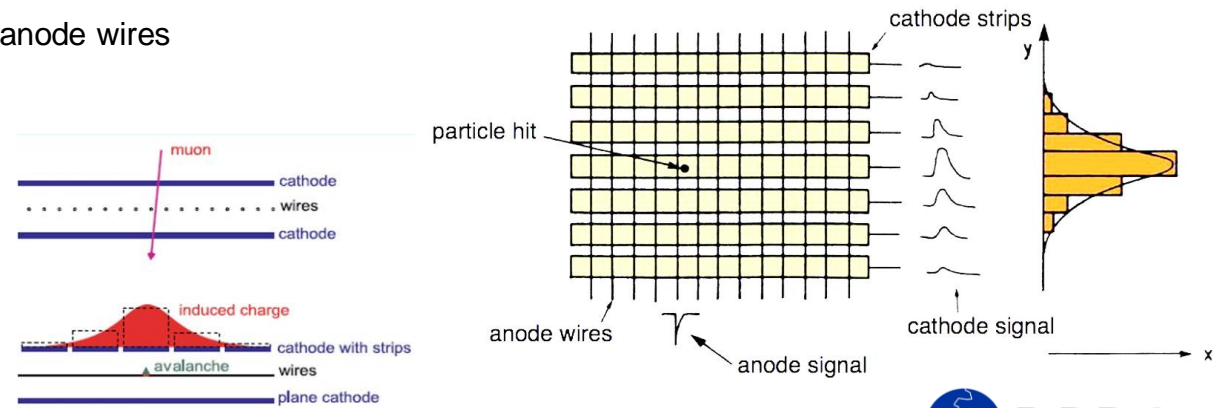
• Drift chamber (1971, 1973*)

- particle tracking with higher spatial resolution: $\sigma \approx 200\mu m$
- field and cathode wires for uniform drift field and adjustable E-field
- larger sensitive gas volume covered per single anode wire than in MWPC
- large-volume drift chambers (e.g. cylindrical) since mid/end of 1980' years
- drift-cell geometries for higher rates (e.g. open and closed cells..)
- drift time measurements yield typical spatial resolutions now of $\sigma \sim 50 - 200\mu m$



• Cathode Strip Chamber (1977*)

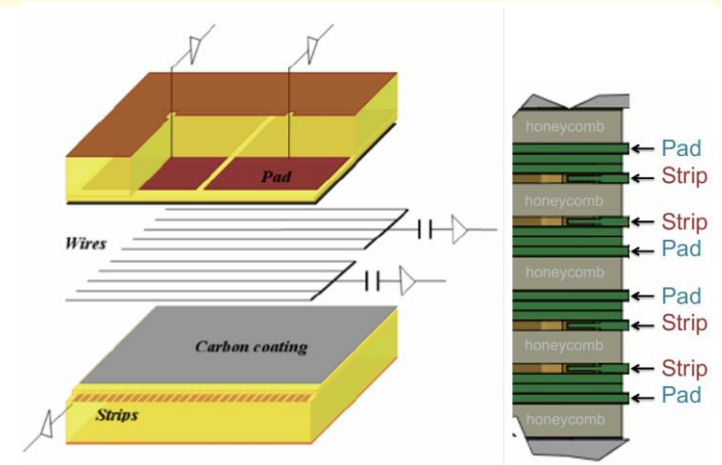
- MWPC measures only track coordinate perpendicular to the anode wires
- 2D track information by segmented cathode (strips) which are perpendicular to anode wires
- measure anode signal and induced signals on cathode strips
- increased spatial resolution by analyzing charge distribution on neighbor strips



1.2 History

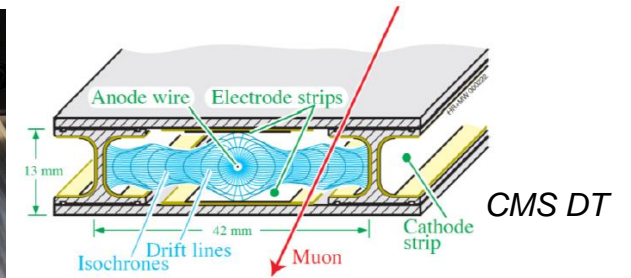
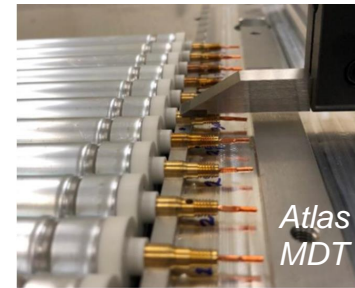
• Thin-Gap Chambers (1983*)

- tracking with much faster timing by very thin gap (~1.4mm) between cathode and anode wire plane
- very small anode wire pitch (~1.8mm)
- very precise alignment of planes required (gaps, wire pitch)
- cathode plane consists of graphite-epoxy mixture, copper strips and pads as readout electrodes
- large sensitive detector area at low cost and high rate capability (together with CSC technology)



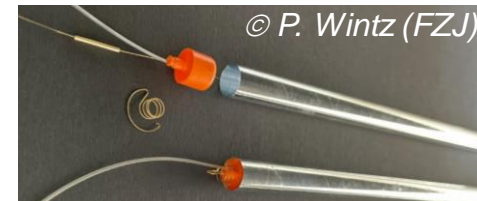
• Drift Tubes (1980)

- drift tubes (DT) or drift cells deliver high spatial resolution ($\sigma \sim 100\mu\text{m}$)
- can cover large sensitive detector area at low costs
- robust mechanics, e.g. honeycomb cells or solid aluminium tubes (~400 μm wall)
- now often as outer muon detectors (CMS, Atlas, ..)

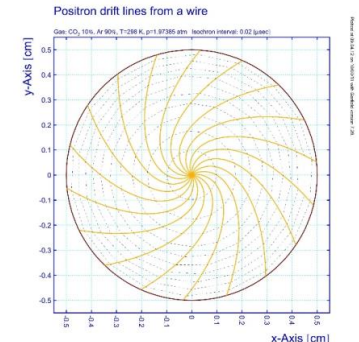


• Straw Tube Chambers (1989)

- anode wire in center of cathode tube, thin metallized film tubes (<30 μm wall) used nowadays
- perfect electrostatic shielding of wire and a broken wire is confined in a single tube
- robust mechanics if at over-pressure, can be operated in vacuum (large gas volumes possible)
- cylindrical geometry with high symmetry: radial distance to wire is the measured quantity



Straw components and e^- drift line simulation (Garfield). Spiral paths due to Lorentz-force by B-field.



2.1 Gas Ionization

• Ionization

- charged particle ionizes the gas along its trajectory and loses energy (dE/dx)
- production of e^- /ion pairs is Poisson distributed ($P(n, \langle n \rangle)$)
- e.g. Ar/CO₂ @ $p=2\text{bar}$: $\sim 170\mu\text{m}$ mean cluster distance, $n_p \sim 60\text{ IP/cm}$, $n_t \sim 190\text{ IP/cm}$
- mean energy-loss (dE) for charged particle (dx =track path length) given by

Bethe-Bloch: $\langle -\frac{dE}{dx} \rangle = K z^2 \left(\frac{Z}{A}\right) \frac{1}{\beta^2} \left[\frac{1}{2} \ln\left(\frac{2m_e c^2 \beta^2 \gamma^2 T_{max}}{I^2}\right) - \beta^2 - \frac{\delta}{2} \right]$

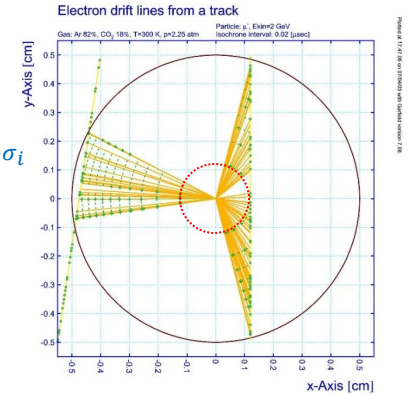
$\langle -\frac{dE}{dx} \rangle \propto \frac{1}{\beta^2}$ up to $\beta\gamma \cong 1$, min. at $\beta\gamma \cong 3$

$P(n, \langle n \rangle) = \frac{\langle n \rangle^n e^{-\langle n \rangle}}{n!}$ with $\langle n \rangle = L/\lambda$, $\lambda = 1/\rho\sigma_i$

$\langle n_t \rangle = L \cdot \left\langle \frac{dE_i}{dx} \right\rangle / W_i$

L = layer thickness, $n_T \sim 2-6 \times n_p$
 λ = mean free path between ionisation
 ρ = density, σ_i = ionization cross-section
 W_i = energy-loss per ionization

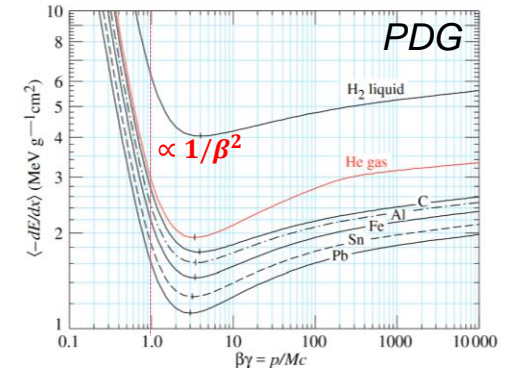
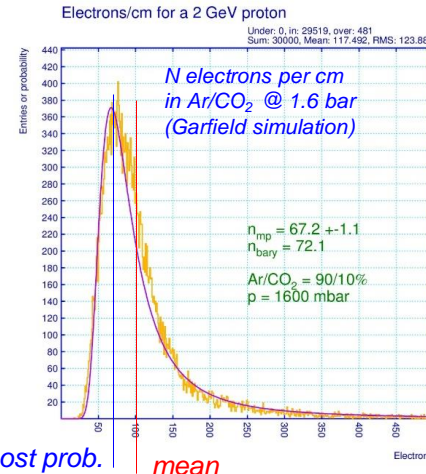
$K = 4\pi N_A r_e^2 m_e c^2$
 I : mean excitation energy
 δ : density effect correction ($\delta = 0$ for mip)



Ionisation clusters along charged particle track path and e^- drift lines (orange).

- dE/dx fluctuates: Landau-distribution with long tail by δ -electrons and secondary ionizations
- mean and most probable dE/dx differ \rightarrow truncated mean is better estimator
- empirical method: truncate $\sim 15-50\%$ of highest entries (= tail) in track sample
- then $dE/dx|_{trunc}$ is shifted, but more Gaussian-like distributed and

most prob. $\frac{dE}{dx}|_{trunc} \cong \text{mean} \frac{dE}{dx}|_{trunc}$

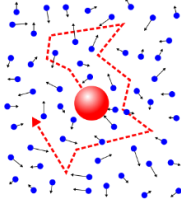


dE/dx as a function of $\beta\gamma$ in helium gas (red line) and different materials

2.1 Drift Motion

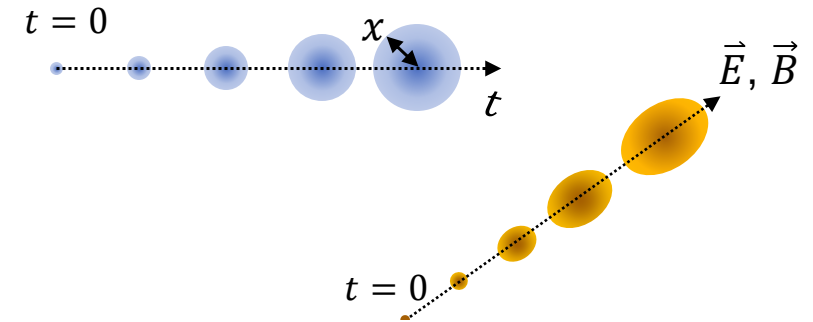
• Gas diffusion

- created ions and e^- lose energy in multiple collision with gas molecules and reach disordered thermal motion (Brownian)
- if started from a point, spatial distribution by diffusion is Gaussian-like with width: $\sigma_x = \sqrt{2Dt}$ and $\sigma_{vol} = \sqrt{6Dt}$
- diffusion coefficient (D) is defined by the mean free path length (λ): $D = \frac{1}{3} v_{th} \lambda$ and $\lambda = \frac{kT}{\sqrt{2}\sigma p}$, mean thermal velocity $v_{th} = \sqrt{8kT/\pi m}$



• Drift motion in E-field

- E-field between anode and cathode accelerate e^- to anode, ions to cathode
- extra velocity affects diffusion in longitudinal (=E-field) direction, transverse unchanged
- frequent collisions with gas limits drift velocity (reaches equilibrium)
- mean drift velocity: $\vec{v}_{dr} = \mu \cdot \vec{E} \cdot \frac{p_0}{p}$, typical values $O(10\mu m/ns)$ for e^- , $O(10\mu m/\mu s)$ for ions (1/1000)

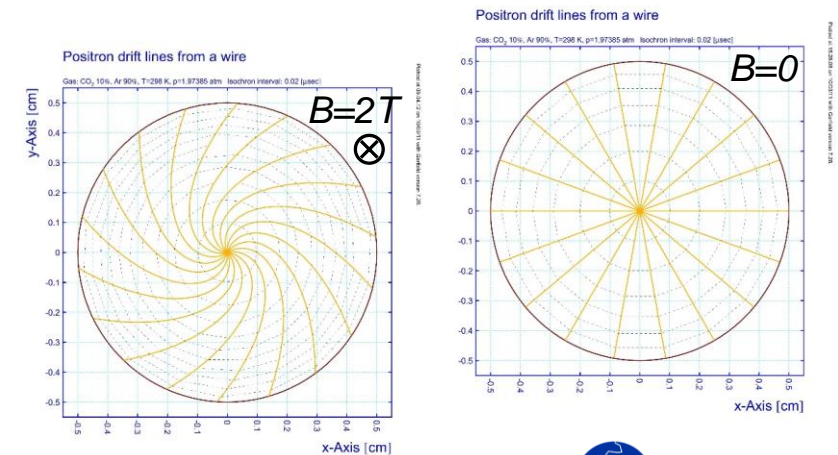


• Presence of B-field

- Lorentz force adds perpendicular velocity component ($\vec{F} = q \cdot \vec{v} \times \vec{B}$)
- different effects on longitudinal and transversal diffusion (σ_{tr} can be reduced if $\vec{E} \parallel \vec{B}$)

• “Cold” and “hot” drift gas

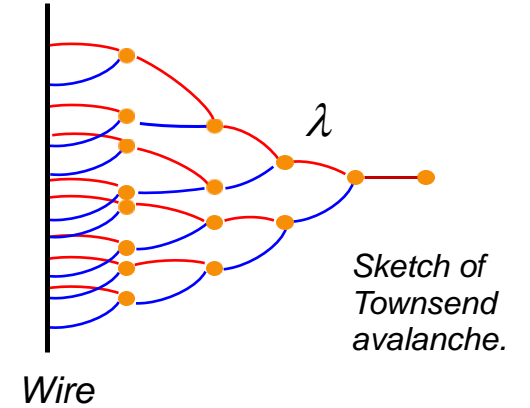
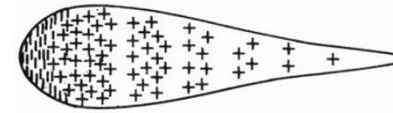
- cold gas approximation ($T_{kin} \sim kT$): $v_{dr} \propto E/p$ and $\mu = const.$
- hot gas approximation ($T_{kin} \gg kT$): $v_{dr} = const.$ and $\mu \neq const.$



2.2 Amplification

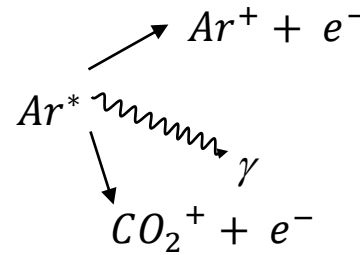
• Gas amplification (Townsend)

- strong acceleration of electrons by rising high E-field ($\propto 1/r$) close to the wire and Coulomb collisions with gas atoms
- probability of an ionization per unit length: $\alpha = 1/\lambda_{ion}$ ($\alpha = 1^{st}$ Townsend coefficient, $\lambda_{ion} =$ mean free path length)
- higher mobility of electrons than ions (1/1000) leads to drop-like shape of avalanche
- gain factor: $G = n/n_0 = e^{\alpha(E)x}$ ($dn = n \cdot \alpha \cdot dx$, $n = n_0 e^{\alpha x}$)
- sparking (streamer) starts at Raether limit: $G \approx 10^8$ ($\alpha x < 20$)



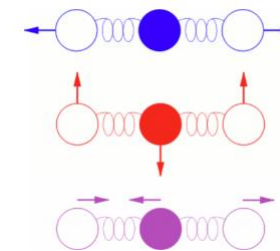
• Penning effect on gas amplification

- excited atoms can further ionize the gas, e.g. argon – CO₂ gas:
- to be added to gain factor, but gas specific

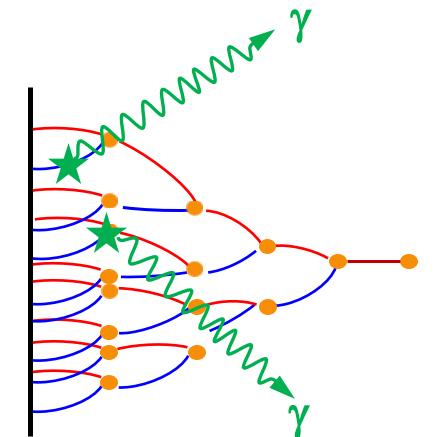


• Quenching of avalanche amplification

- UV-photons (γ) can be produced during avalanche process
- can start (unwanted) new ionization in the gas or photo-emission from cathode
- add “quench” gas as admixture, molecules with vibration excitation modes to absorb photons
- e.g. carbon-dioxide, CO₂ is linear molecule (O-C-O) with vibration modes (see sketch)
- carbohydrates, complex molecule chains with many more vibration and rotation modes; better quencher, but polymerization possible (can cause ageing)



CO₂ vibration modes (picture from Piet V.).



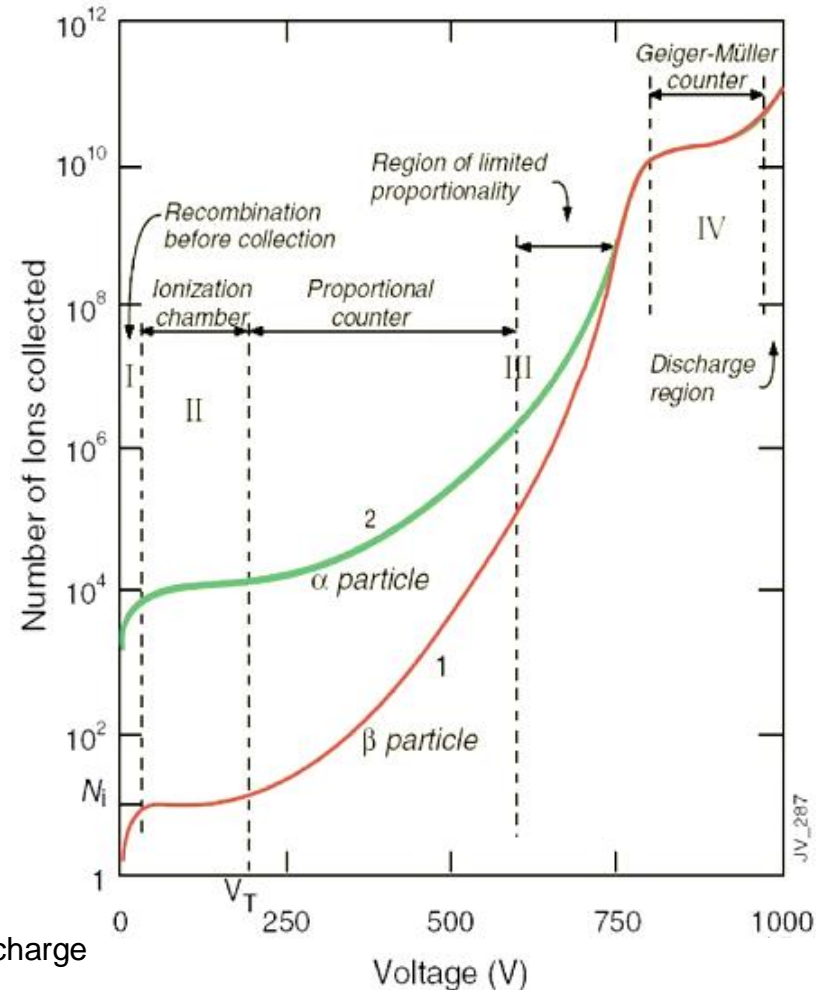
UV-photon production during avalanche process.

2.2 Operation Modes

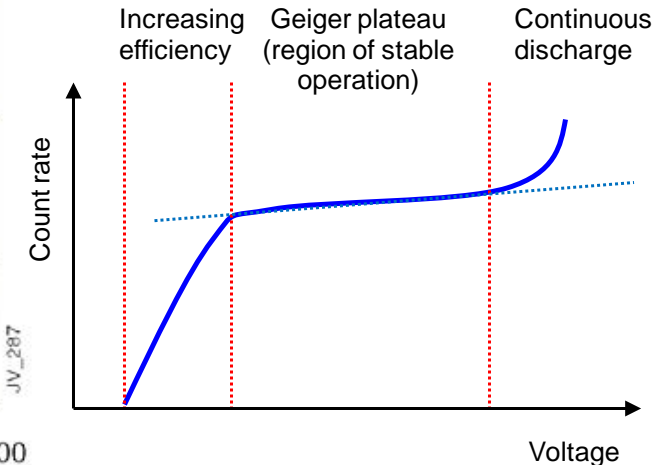
• Operation modes

(gain factor G : number collected e^- per primary ionization e^-)

- **Ionization chamber**
 - full charge collection, no charge multiplication
- **Proportional counter ($G \approx 10^4 - 10^5$)**
 - avalanche and signal proportional to primary ionization
 - dE/dx measurement possible
 - quenching of avalanche-created UV-photons
- **Limited proportional mode (G up to $\approx 10^8$)**
 - strong photo-emission with further ionizations
 - stronger quenchers required or pulsed HV
- **Geiger mode**
 - very strong photo-emission, ionization over full volume
 - discharge to be stopped by HV breakdown
- **Discharge**
 - streamer building between electrodes with complete discharge



High voltage characteristics for a const. irradiation source

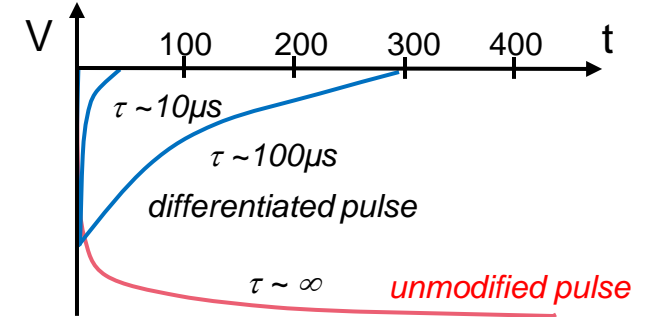


- **“Geiger plateau”** measurement to determine high voltage region of stable detector operation in proportional mode (lab course)

2.3 Signal Readout

• Induced signals

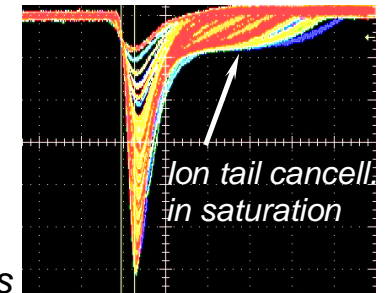
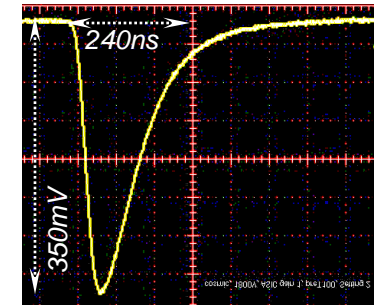
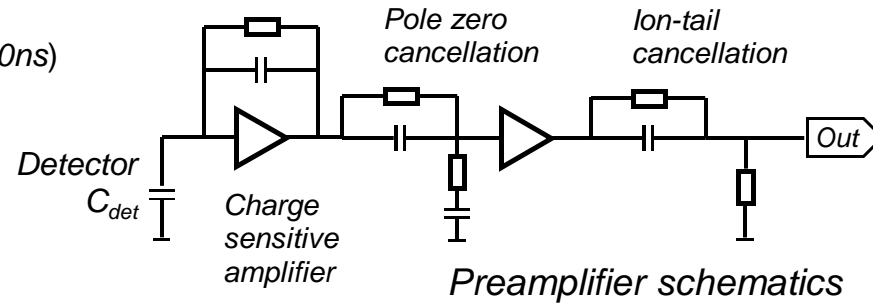
- the charges moving in the E-field between the electrodes induce signals on anode wire and cathode
- most of the electron-ion pairs are created close to the anode wire in the avalanche process ($A \sim 10^{4-5}$)
- most contribution to the induced charge signal is due to the slower ion movement ($1/1000 \times e^-$)
- signal has to be electronically differentiated to have reasonable time response and low deadtime



(F. Sauli, ebook: [10.5170/CERN-1977-009](https://cds.cern.ch/record/10.5170/CERN-1977-009))

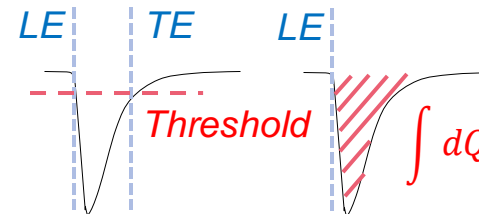
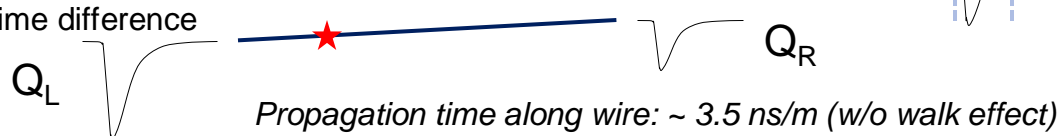
• Charge sensitive amplifier with signal shaping

- signal amplification (e.g. 1-4 mV/fC, typical peaking times 5-50ns)
- preamplifier pole zero cancellation
- ion tail cancellation (typical signal width < few 100ns)
- baseline restoration for high rate capabilities (~ MHz)



• Signal information

- Leading-edge (LE) and trailing-edge (TE) time, time-over-threshold (TE-LE)
- integrated charge signal shape (e.g. sampling ADC)
- readout at both wire ends can locate signal creation along wire ($\Delta t, \Delta Q$): charge division, time difference



Signal examples (measurements, Panda-type straws).

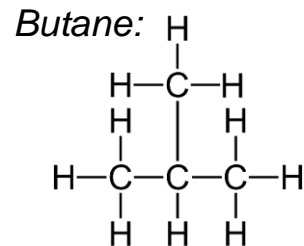
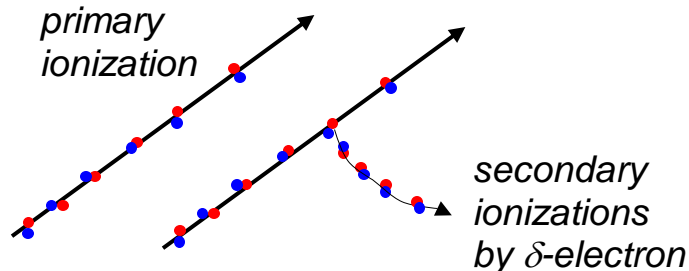
2.4 Drift Gas

Important properties and characteristics

- ionization density (n_t = total IP per unit length) and radiation length (X_0)
- basic drift gases: inert gases
- added quench gases: CO₂ (“clean”), carbohydrates (“very efficient”)
- O₂ small admixture (electro-negative!) to mitigate ageing

Selection criteria

- high ionization density and high radiation length (X_0) preferable
 - He for low multiple scattering ($\propto Z^2$)
 - Xe for high ionization density ($\propto Z$) and X-ray detection (TR), but expensive
 - Ar frequently used as drift gas basis
- drift velocity characteristics, low diffusion and low Lorentz-angle in E-, B-field
- sufficient quenching for localized amplification avalanche and stability
- examples of typical gas mixtures: Ar/CO₂(10-50%), He/i-C₄H₁₀, ..



Quench gases

$$n_t = \frac{dE}{W_i} \text{ and } n_t \approx 2 \dots 7 \cdot n_p$$

*dE: total energy loss,
W_i: avg. energy loss per ionization
I₀: avg. ionization energy (Bethe Bloch)*

Gas	Density* [g/cm ³]	I ₀ [eV]	W _i [eV]	dE/dx [keV/cm]	n _p [IP/cm]	n _t [IP/cm]	X ₀ [m]
H ₂	8.38 x10 ⁻⁵	15.4	37	0.34	5.2	9.2	7522
He	1.66 x10 ⁻⁴	24.6	41	0.32	5.9	7.8	5682
N ₂	1.17 x10 ⁻³	15.5	35	1.96	(10.0)	56.0	325
O ₂	1.33 x10 ⁻³	12.2	31	2.26	22.0	73.0	257
Ne	8.39 x10 ⁻⁴	21.6	36	1.41	12.0	39.0	345
Ar	1.66 x10 ⁻³	15.8	26	2.44	29.4	94.0	118
Kr	3.49 x10 ⁻³	14.0	24	4.60	22.0	192.0	33
Xe	5.49 x10 ⁻³	12.1	22	6.76	44.0	307.0	15
CO ₂	1.86 x10 ⁻³	13.7	33	3.01	34.0	91.0	183
CH ₄	6.70 x10 ⁻⁴	13.1	28	1.48	16.0	53.0	646
C ₂ H ₆	1.34 x10 ⁻³	11.7	27	1.15	41.0	111	340
C ₄ H ₁₀	2.42 x10 ⁻³	10.8	23	4.48	(46.0)	195	169

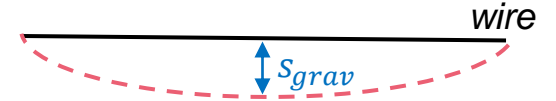
*at STP

K, Kleinknecht, Detektoren für Teilchenstrahlung, B.G. Teubner, 1992;
F. Sauli, ebook: [10.5170/CERN-1977-009](https://cds.cern.ch/record/10.5170/CERN-1977-009)

2.5 Wire Aspects

• Precise wire position required

- anode wire in center of cathode tube or in center of drift cell with surrounding field/cathode wires
- in anode wire plane and between cathode planes
- position distortion limits measurement precision (time, charge) and electrostatic stability
- E-field distortion by off-centered anode wire, affects gas gain and space-drift time relation



$$s_{grav} = \frac{L^2 g \rho \sigma}{8 T} \propto L^2$$

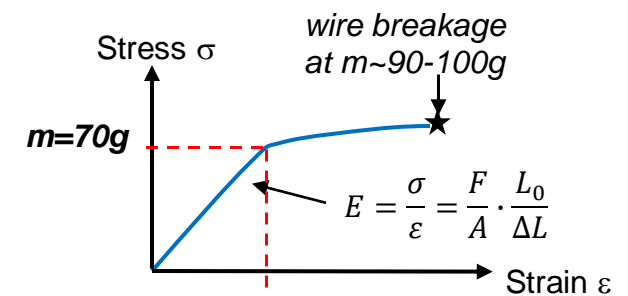
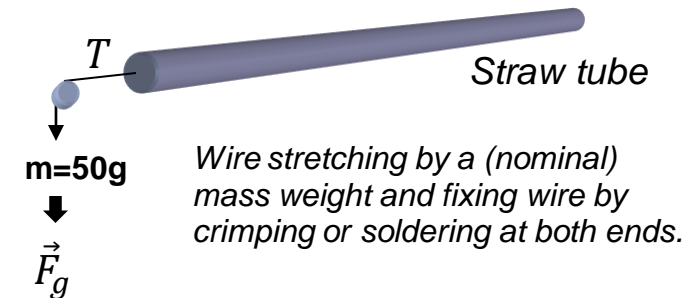
(e.g. $s \sim 35\mu\text{m}$ for $L=1.4\text{m}$, $F=0.5\text{N}$, $20\mu\text{m}$ diam.)

• Wire position distortion by

- electrostatic repulsion between anode wires, only for perfect geometry anode wire in equilibrium
- sag (s_{grav}) for horizontal wire due to gravitational force. $s_{grav} \propto L^2$ ($L = \text{wire length}$)
- mechanical imperfection (assembly quality, material relaxation, ..)

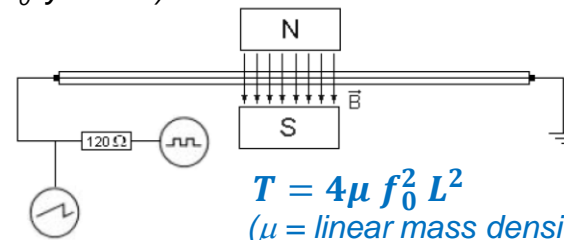
• Mitigation: stretch wire from both ends

- tension (T) must be high enough to achieve wire stability and to reduce gravitational sag, but
- below inelastic wire stretching region (e.g. $F < 0.7\text{N}$ for $20\mu\text{m}$ diameter W/Re wire)
- above critical minimum tension T_c for electrostatic stability
- tension check method: measure the wire oscillation frequency (1^{st} harmonic f_0 yields T)



$$T \geq T_c = \left(\frac{U_0 \cdot l}{d}\right)^2 \cdot 4\pi\epsilon_0 \left[\frac{1}{2\left(\frac{\pi L}{d} - \frac{2\pi r_w}{d}\right)}\right]^2$$

(e.g. $T_c \sim 0.5\text{N}$ for drift cell $l=1\text{m}$, $d=2\text{mm}$, $r_w=15\mu\text{m}$, $L=10\text{mm}$, $U_0=5\text{kV}$)



2.5 Wire Aspects

- **Wire materials** (typical)

- tungsten or tungsten-rhenium(few %) alloy, for anode wire, typical 20-30 μ m diameter
- gold-plated for surface inertness
- aluminium for field or cathode wires with bigger diameters, typical 50-100 μ m diameter, high radiation length

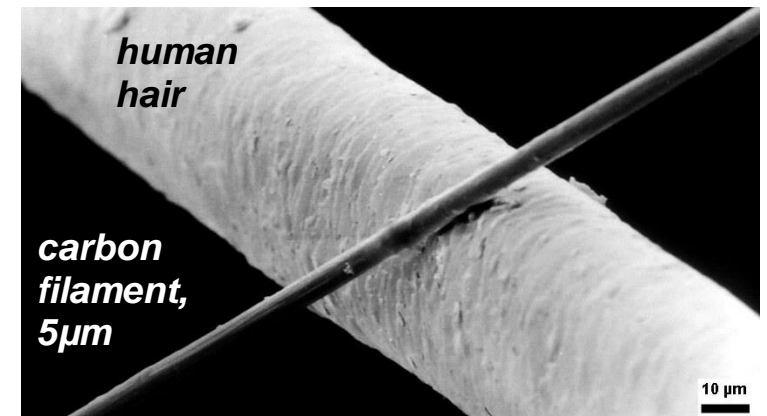
- **Wires in drift chamber cell**

- cell consisting of anode and cathode wires with different materials and diameters
- precise same horizontal sag over large length (up to 4m) is required for electrostatic stability
- exact tension for anode and cathode has to be calculated and provided by the mechanical frame

- **Wire R&D ongoing**

- drift chamber with 100.000' of wires, further optimization of wire strength and high radiation length
- "standard" wire materials are tungsten, rhenium and aluminium
- aluminium wires can undergo corrosion (humidity)
- further materials under study for low material budget (X/X0) of the detector
- carbon (mono-)filaments, metallization, .. roundness difficult
- beryllium, expensive, machining difficult (toxic)

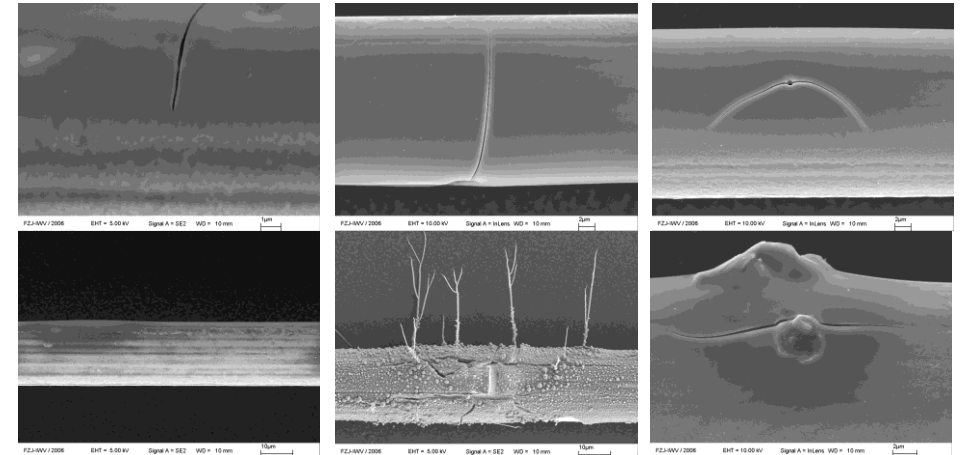
Element	X_0 (cm)
Beryllium	35.28
Carbon	21.35
Aluminium	8.897
Iron	1.757
Molybdenum	0.9593
Tungsten	0.3504
Rhenium	0.3183
Gold	0.3344



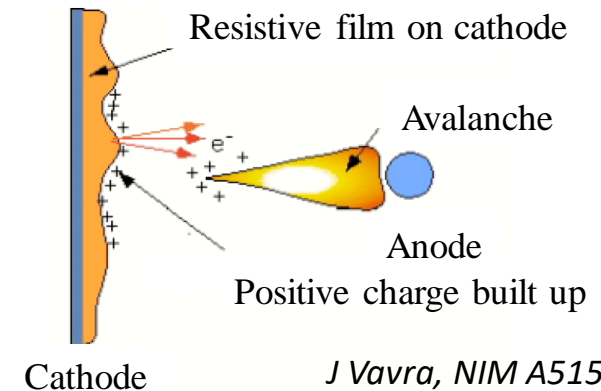
2.5 Ageing

- **Ageing effects** by deposits on electrodes
 - inefficiency: gas gain reduction ($\Delta G/G_0$), can be local or spread by gas flow
 - HV instability: self-sustaining currents caused by deposits on wire or cathode
 - longevity parameter: total accumulated charge on wire per unit length (C/cm)
- **Avalanche formation creates a micro-plasma**
 - possible chemical reaction: formation of radical molecules, polymerization (whiskers), ..
 - created polymers can attach to electrodes (deposits) and distribute by gas flow
 - even traces (ppm) of gas pollution is dangerous, outgassing of materials
 - wire quality, e.g. Au-plating porosity: wire oxidation \rightarrow wire swelling \rightarrow gain drop
- **Mitigation**
 - avoid contamination: from assembly and materials (e.g. glue) or improper materials cleaning
 - avoid contamination from (uncleaned) gas system components (e.g. lubricants, oil, silicon..)
 - no excessive gas gains (e.g. limited streamer mode at $A > 10^5$), can cause accelerated ageing
- **Recipes to cure existing ageing**
 - additives: oxygen (few%), water (traces) to cure ageing by chem. reaction with deposits
 - recently: *3rd International Conference on Detector Stability and Aging Phenomena in Gaseous Detectors, CERN, 2023*

Other material “ageing” effects (relaxation, corrosion, ..) not discussed here..



Scanning Electron Microscopy (SEM) of wire (P. Wintz, FZJ). Top: non-irradiated wire with gold-plating imperfections. Bottom: irradiated wires with deposits (C, Si, whiskers, ..).



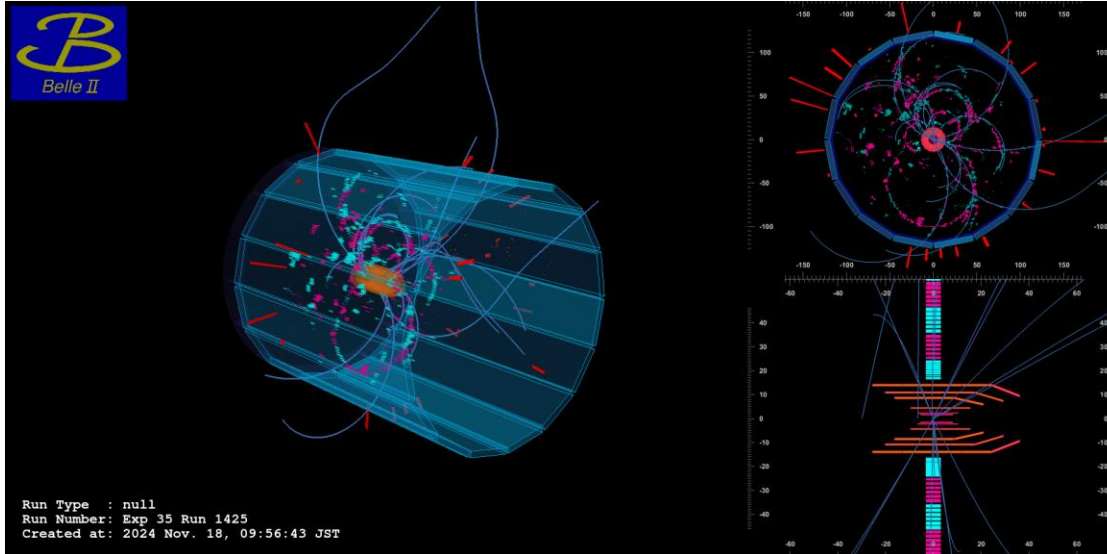
J Vavra, NIM A515 (2003)

Secondary electron emission by resistive film creation on cathode with accumulation of large positive charge (Malter effect, Phys. Rev. 50 (1936) 48.).

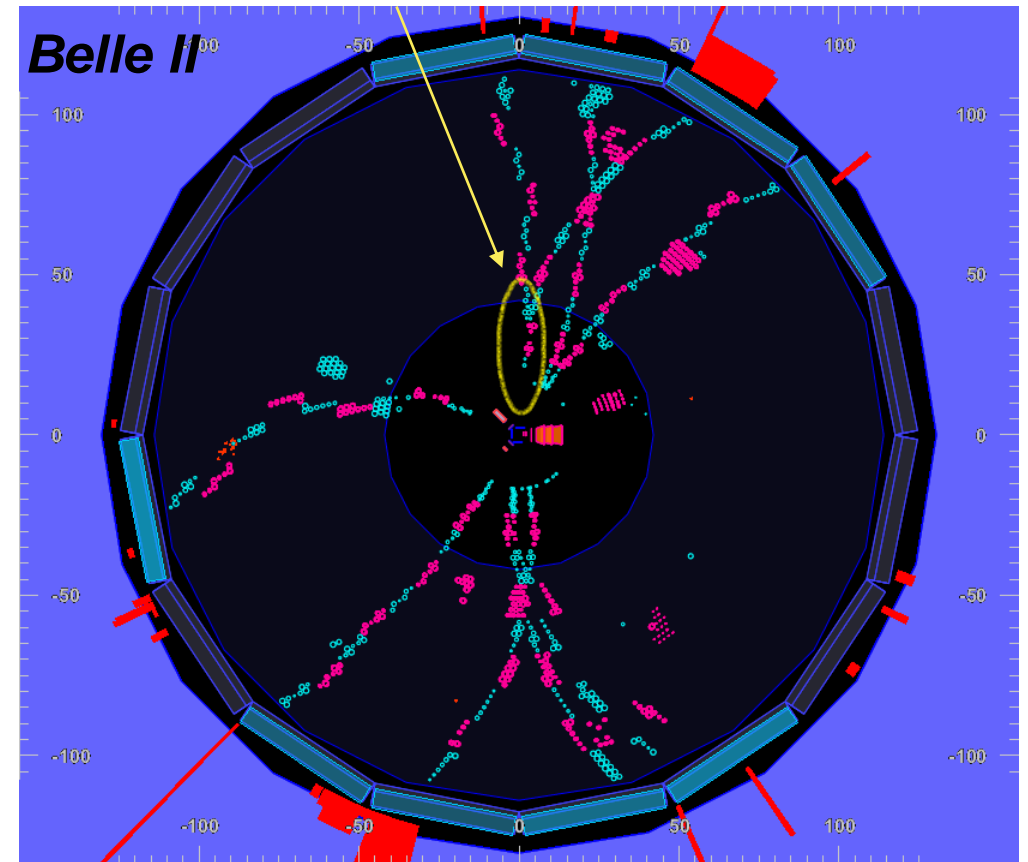
3. Measurements and Resolutions

- Drift time for spatial information and particle trajectory reconstruction
- Particle momentum from trajectory in B-field (e.g. curvature)
- Particle specific energy-loss (dE/dx) for PID
- Time information for crossing particle
- Often: continuous data stream and online reconstruction
- Input to SW-trigger (realtime event selection)

Belle II: Event Display (many thanks for public accessibility!)



Event with reconstructed $K_S^0 \rightarrow \pi^+ \pi^-$ Identified by displaced vertex in Belle II CDC



3.1 Drift Time

- **Space - drift time relation to be determined (calibration)**

- drift tubes with ϕ -symmetry: isochrone radius $r(t)$ is space-time relation
- multiple hit tubes and track fit tangential to isochrones (χ^2 -minimization of distances)

- 1st step: extract drift time from time measurement

$$t_{meas} = t_0 + t_{tof} + t_{prop} + t_{walk} + t_{drift}$$

- 2nd step: reconstruct tracks with space-time relation

(e.g. from time spectrum, or rough by taking wire positions)

- 3rd step: determine reconstructed track space points as input for further iterative $r(t)$ optimization

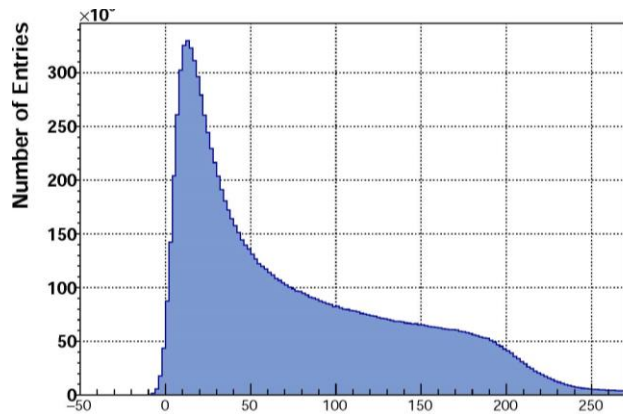
polynomial parametrization of $r(t)$

$$t_0 = t_{ref} \text{ (varies if continuous data stream)}$$

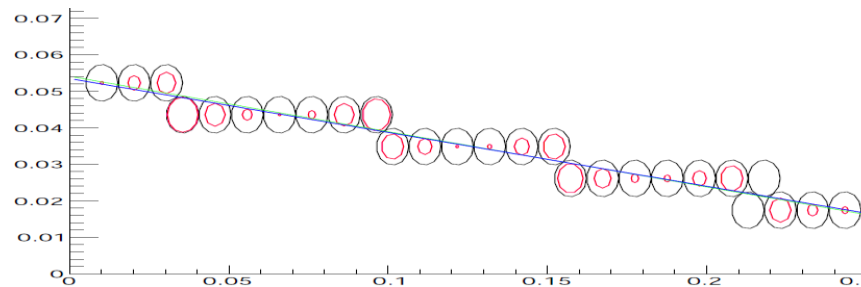
$$t_{tof} = \text{particle time of flight}$$

$$t_{prop} = \text{signal propagation along wire}$$

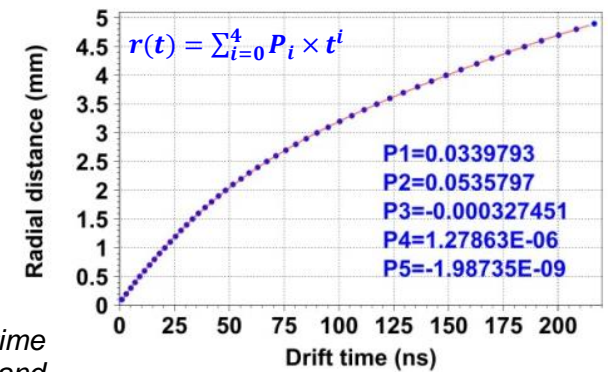
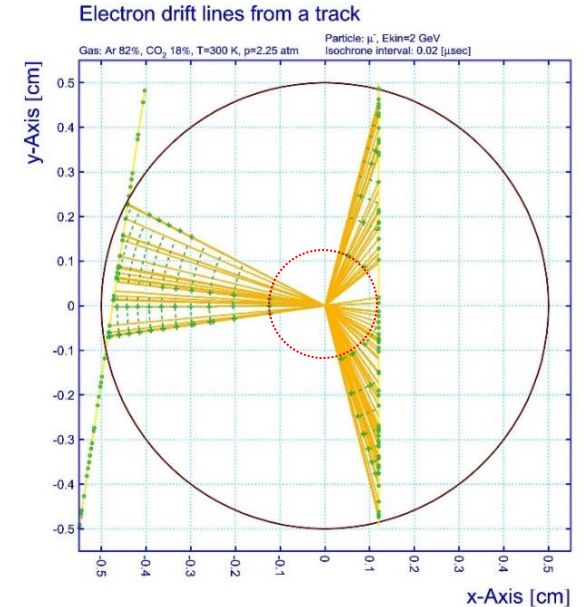
$$t_{walk} = \text{signal time walk}$$



Straw drift time spectrum (in-beam data)

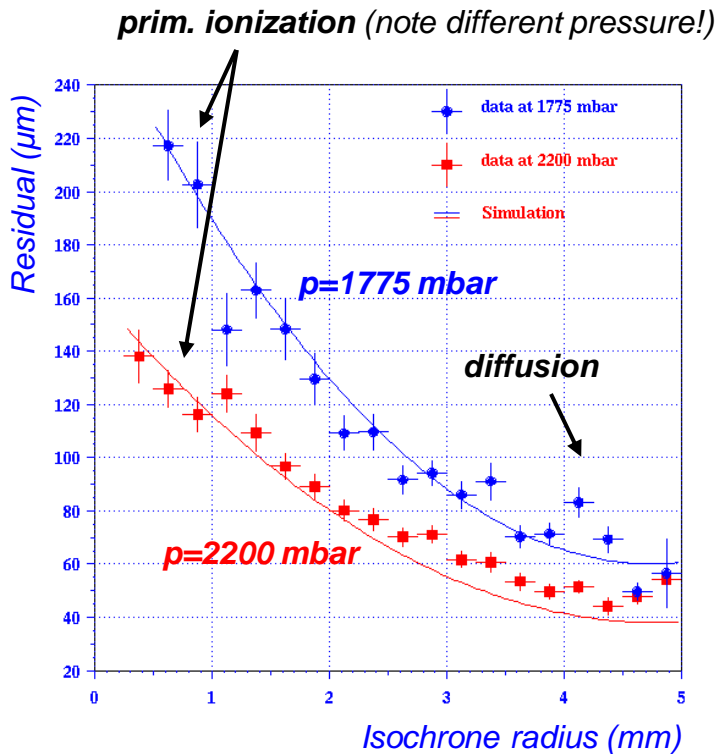


In-beam straw test system with hit straws and measured drift time isochrones (red circles). Pre-fit (green line) of track by wire positions and track fit (blue line) by minimizing distance to the isochrones (χ^2 -fit).

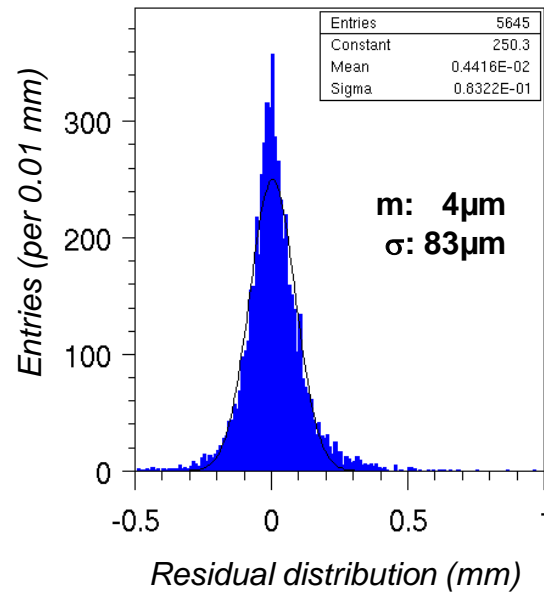


3.1 Spatial Resolution

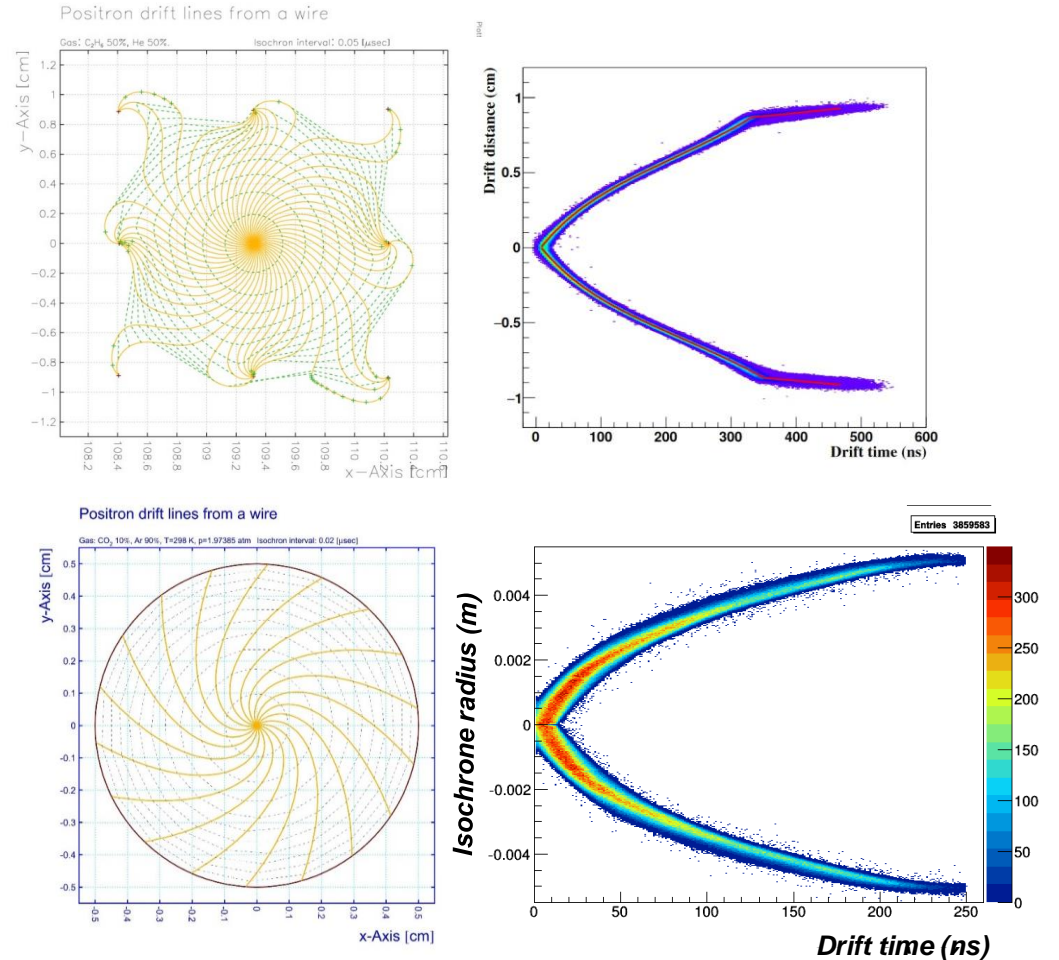
- **Space – drift time relation** depends on cell geometry
- **Spatial resolution** of drift time measurement (σ_t)
 - typical: 50-200 μm (σ), depending on cell geometry, gas, electronics
 - intrinsic smearing: primary ionization close to wire, diffusion dominates at large distance
 - electronics: gain and threshold, time walk



$$\sigma_t = \sqrt{\sigma_{ion}^2 + \sigma_{diff}^2 + \sigma_{elec}^2}$$



Cell geometry and space – drift time relation (in-beam data): Belle-CDC (top row) and PANDA straw tube (bottom row).



3.1 Spatial Resolution

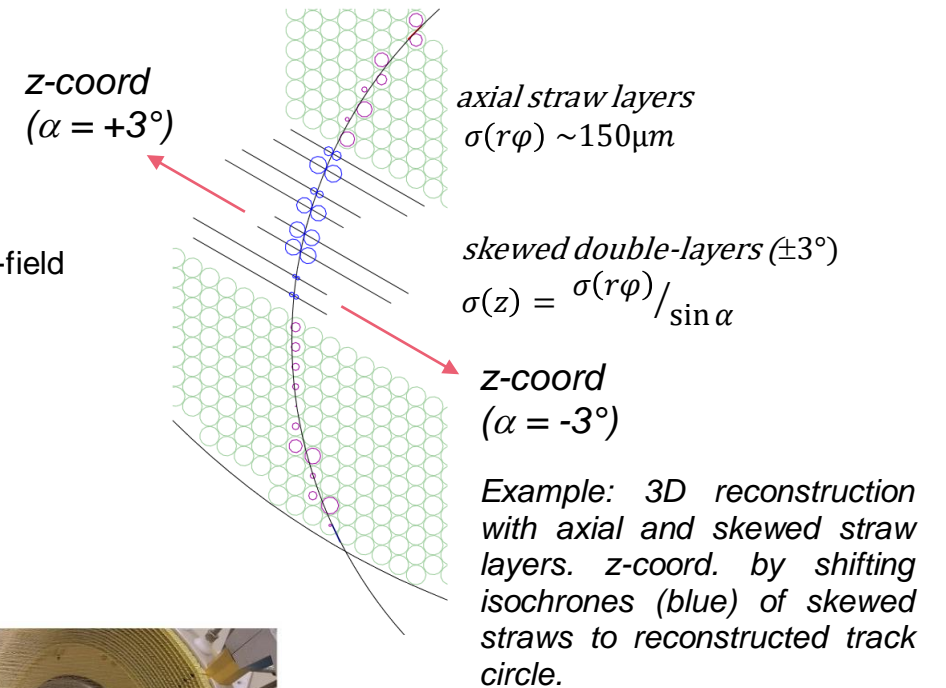
- **2D spatial track information** in plane perpendicular to wire was discussed
- How to get **coordinate of track along wire (3D)**
 - usually defined as “z” coordinate
 - in cylindrical detectors: anode wires are aligned parallel to beamline (=z-axis) and to solenoidal B-field

- **3D track** info by two possible methods

- combination of axial and stereo (skewed) wire layers
 - combination of hit axial and stereo (\pm deg) wires yield z-coordinate
 - typical resolution: $\sigma(z) \sim$ mm, depending on skew angle (α), e.g. $\sigma(z) = \frac{\sigma(r\varphi)}{\sin \alpha}$
- signal readout at both ends of wire
 - charge division and signal propagation time difference along wire yield z-coordinate
 - typical resolution: $\sigma(z) \sim$ cm and \sim 2-3% of wire length

- Planar layer detectors

- e.g. around and inside dipole B-field for momentum reconstruction
- different phi-angles: e.g. $0^\circ, 90^\circ, +45^\circ, -45^\circ$ or $0^\circ, 60^\circ, 120^\circ$
- better more than two phi-orientations to resolve ambiguities



Skewed wires in MEGII drift chamber (left) and straw layers (right) in GlueX CDC straw chamber (N. De Filippis and N. Jarvis, Straw Tracker 2024 mini Workshop).

3.2 Momentum Resolution

- **Charged particle trajectory** in a uniform B-field (e.g. solenoid B-field)

- $p_{tr}[GeV/c] = 0.3 \cdot B[T] \cdot R[m]$ ($\vec{F}_{Lorentz} = \vec{F}_{centrifugal}$)
- $p = p_{tr} / \sin \theta$ (θ : angle to z-axis)
- measure track curvature R which gives transverse momentum
- total momentum from ptr and track angle

- **Resolution:**

$$\left(\frac{\sigma_{pt}}{p_t}\right)^2 = (a \cdot p_t)^2 + b^2$$

↑ ↑
 Detector resolution Multiple scattering

$$a = \frac{\sigma_{r\phi}}{0.3 \cdot BL^2} \sqrt{\frac{720}{N+5}}$$

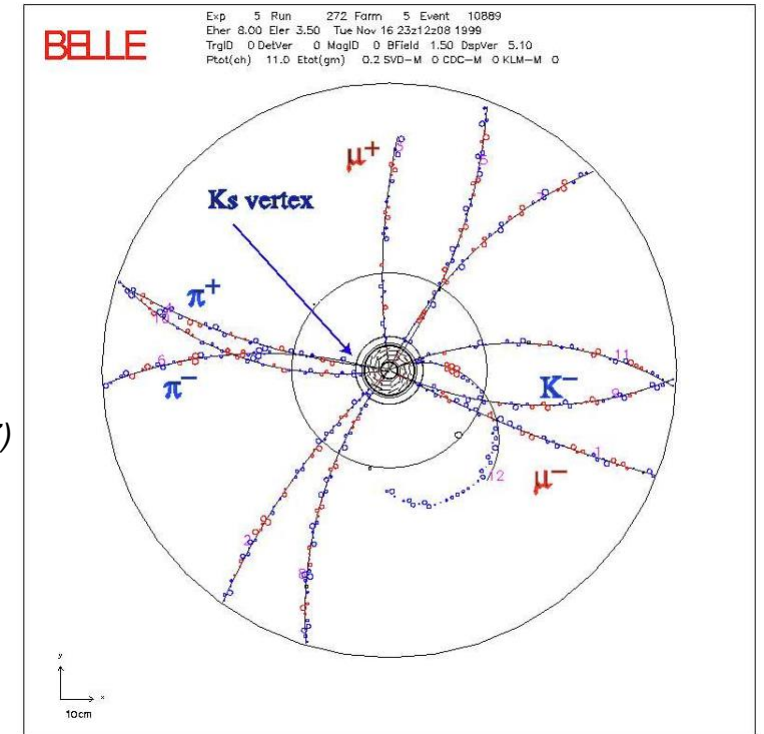
$$b = \frac{0.045}{\beta BL} \sqrt{\frac{L}{X_0}} \cdot \left[1 + 0.038 \cdot \ln \frac{L}{X_0}\right]$$

(Gluckstern, NIM 24 (1963) 381,
 Drasal and Riegler, NIM A 910 (2018) 127)

- $\sigma_{r\phi}$: spatial hit resolution
- p_t : transverse momentum
- B : Magnet field strength
- L : Lever arm (chamber size)
- N : Number space hit points
- X_0 : Radiation length (m) of detector

- degrades linearly with transverse momentum
- improves linearly with B field strength
- improves with detector radial extension (L)
- MS contribution constant over pt and improves by low detector material budget (L/X0)

- **In short: large detector size with many high-resolution hit points and low multiple scattering for high resolution**



Belle CDC with L~800mm lever arm

3.3 Particle Identification (PID)

- **Energy-loss (dE/dx)** in gas by charged particle depends on $\beta\gamma=p/Mc$ (see slide 7)
- measured dE/dx and known (reconstructed) particle momentum gives particle mass (=PID)

• dE/dx measurement

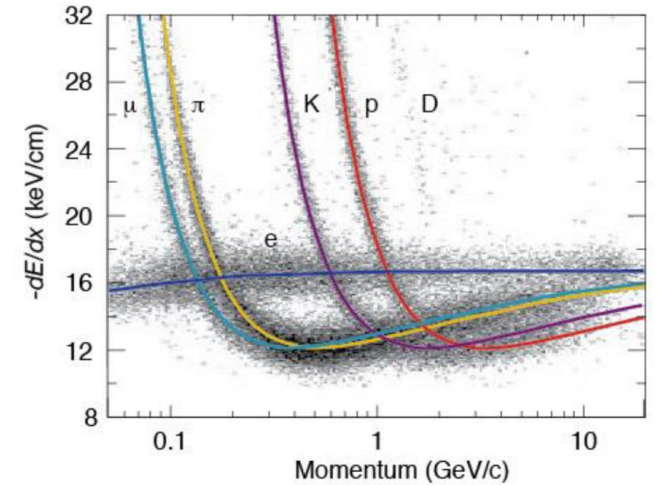
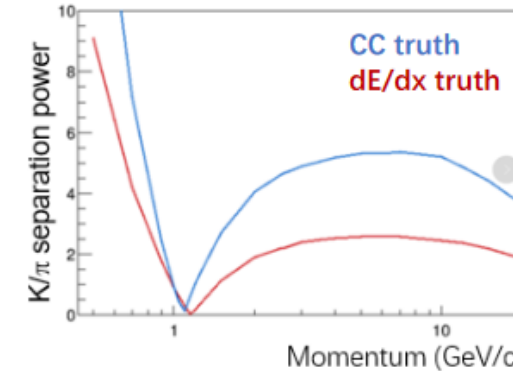
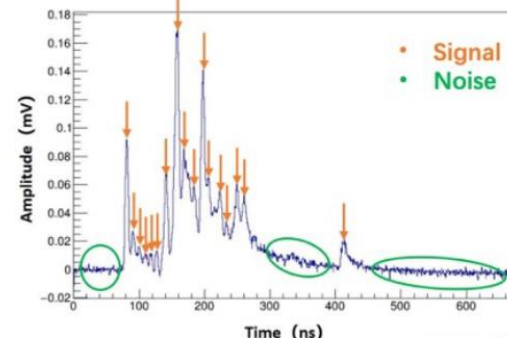
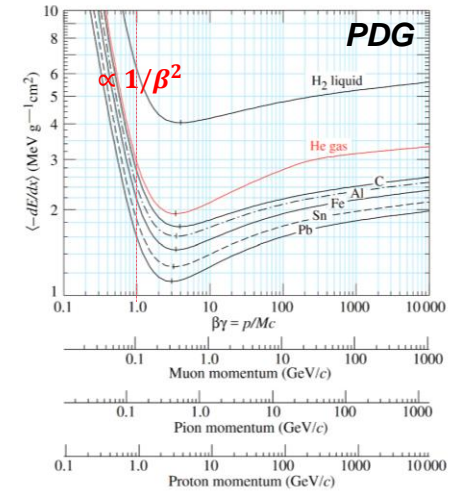
- Landau-distribution: mean and most probable dE/dx differ \rightarrow truncated mean is better estimator (more gaussian-like distributed)
- empirical method: truncate $\sim 15-50\%$ of highest entries (= tail) in track sample
- need high number of sampling points per track for good truncation

• Charge (=dE) measurement methods

- charge signal shape integration (e.g. by sampling ADC)
- charge signal width by time-over-threshold (only time measurement)
- number of ionization clusters ($N \cdot W_i \rightarrow dE, W_i = avg. \text{eloss}/cluster$) (slide 12)

• dN/dx measurement is less established, but promising

- better resolution than for integrated dE/dx (\sim factor two in simulation)
- can allow PID in region $\beta\gamma > 3$ GeV/c due to sharper relativistic rise
- needs fast and very sensitive electronics to resolve single clusters
- (realtime) efficient, fast peakfinder algorithm and training with data (e.g. ML)



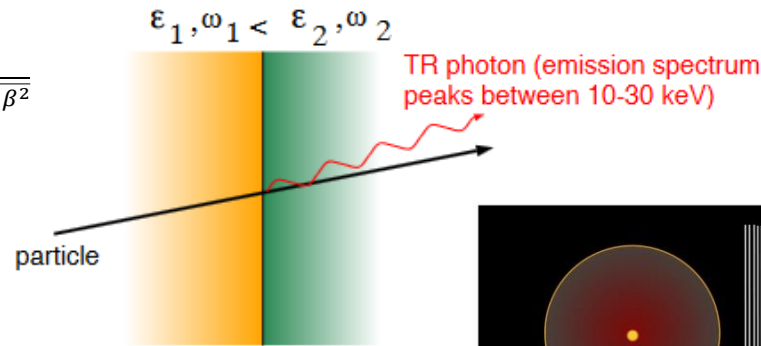
Measured dE/dx and momentum for different particle species (PEP-4 TPC at SLAC, gas pressure 8.5 atm).

Cluster counting (CC) and K/π separation power for dE/dx and CC (simulation, G. Zhao, DRD1 meeting 2024/1).

3.3 Particle Identification

• **Transition radiation (TR)** in X-ray energy region is created when a relativistic charged particle crosses the boundary of two media with different dielectric constants

- Intensity of transition radiation (TR) scales with γ : $I \propto m\gamma = m \frac{1}{\sqrt{1-\beta^2}}$
- TR photon angle has sharp maximum at $\theta \sim 1/\gamma$
- TR very efficient for electron identification with $\gamma \sim O(1000)$



• Detector signal

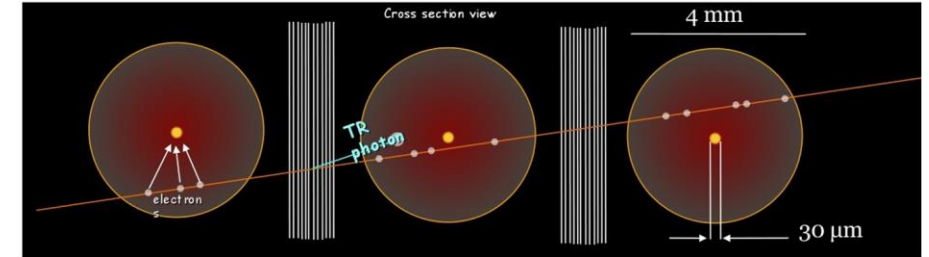
- charged particle ionization (~few keV/cm) and
- gas ionization by TR photon with energy in range of ~10-30keV

• Detector layout

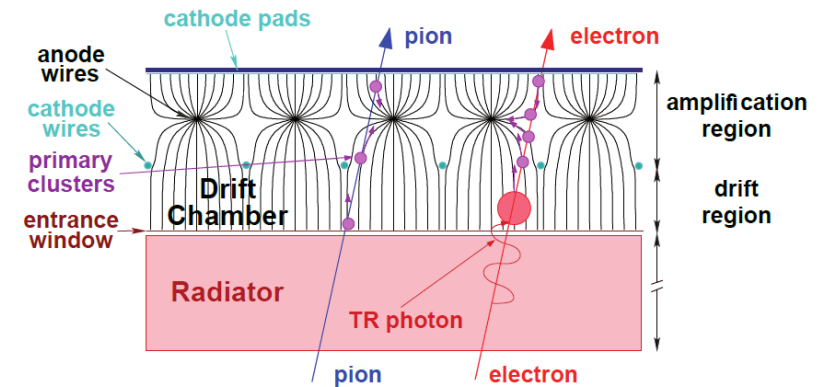
- gas ionization volume with thin foils
- TR media in front
- many transition layers for sufficient TR probability, e.g. stack of foils, fibers, ..
- Xe gas used in most cases, has high ionization and TR absorption probability

• Very efficient electron-hadron separation

- but xenon is expensive → closed gas circuit and Xe recuperation needed
- charged particle and X-ray signal identification needed (e.g. 2-threshold method, low+high threshold)



Sketch of Atlas TRT straw tracker



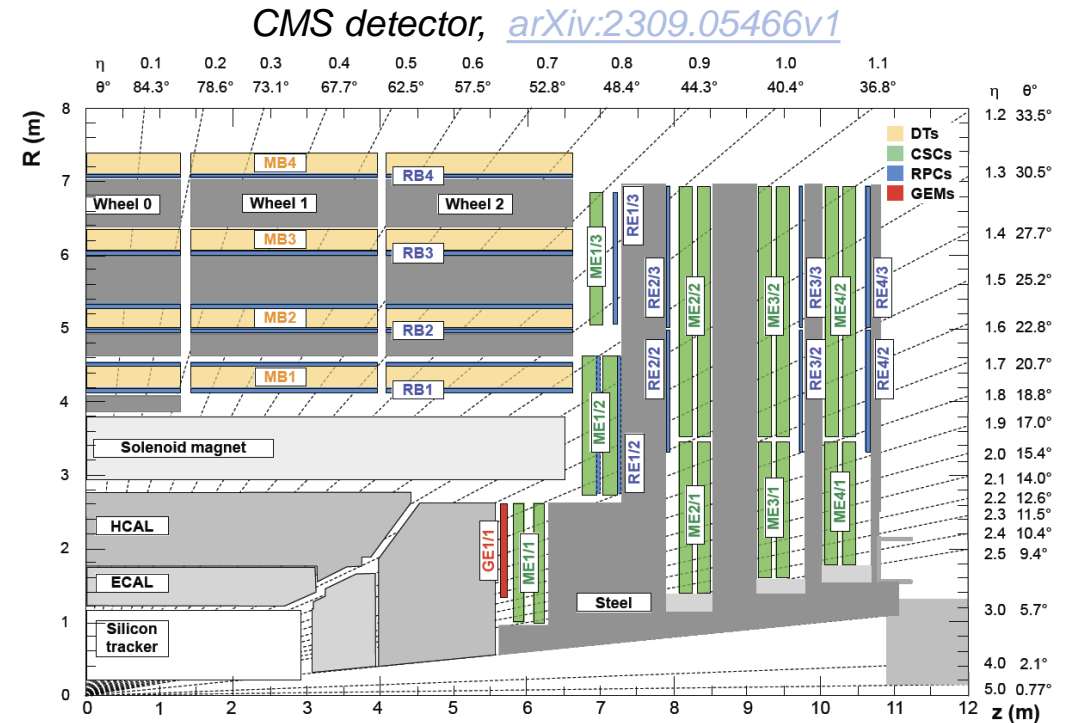
Sketch of the MWPC for the CBM at FAIR experiment (from F. Fidorra, IKP, Univ. Münster).

4. Detectors and Applications

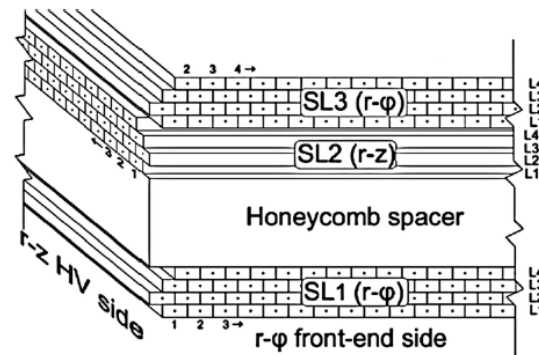
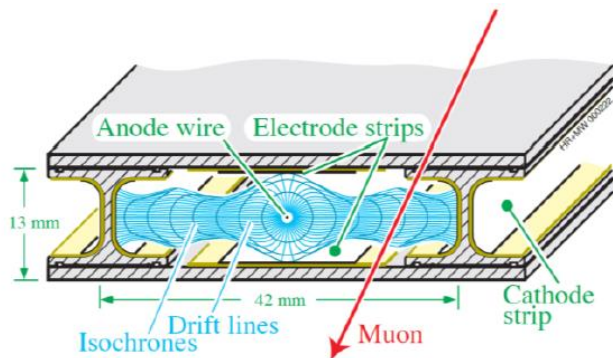
- Experiments with wire-based detector systems ranging from
 - HEP (e.g. CMS, Atlas, LHCb, Belle, future FCC-ee/hh, ..)
 - Hadron physics (NA62 at CERN , CBM & PANDA at FAIR)
 - Dark sector (SHiP at CERN)
 - Rare decay experiments (Mu2E, Comet)
 - Neutrino physics (DUNE)
- Detector systems
 - Drift tubes, MDT
 - Straw trackers
 - TR Straw tracker
 - Vacuum straw tracker
 - Drift chambers
 - Cathode-Strip-Chamber
 - Thin-Gap-Chamber
- Discussion of current or planned wire-based detector systems in experiments on next slides

4.1 Drift Tubes at CMS

- **Part of Muon System**, which consists of DT, CSC, RPC, GEM
 - Tasks: muon tracker, PID, momentum
 - Input for trigger, luminosity monitoring
 - **172,000 rectangular cells** ($4.2 \times 1.3 \text{ cm}^2$), area: **18,000 m²**
 - 100 μm spat. resolution, high segment reco efficiency (>99%)
- **Originally: 10y LHC lifetime foreseen**
- **Further use in HL-LHC**
 - Preparations: ageing and reco. efficiency studies done (GIF++)
 - Acceptable efficiency degradation (redundancy)
 - Ageing mitigation (e.g. O₂, H₂O, lower HV)
 - Readout electronics upgraded (on-board, backend, ..)



Parameter	Value
Rectangular cell	$4.2 \times 1.3 \text{ cm}^2$
Wire diameter	50 μm Steel / Au-plated
Gas	85/15 Ar/CO ₂
Gas pressure	3 mbar Overpressure
Number channels	172,000
Number chambers	250 8 \times r ϕ , 4 \times r z per chamber
Surface area	18,000 m ²
Spat. resolution	$\sim 100 \mu\text{m}$ (σ)
Time resolution	2 ns



4.2 Cathode Strip Chambers

At CMS and ATLAS

CSC: grid of anode wires and cathode strips [\[14\]](#)

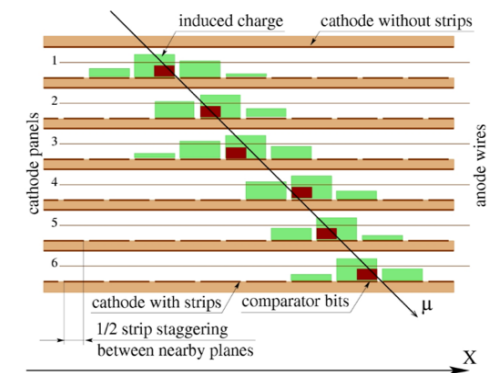
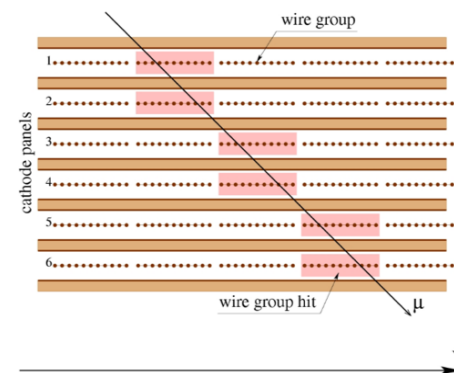
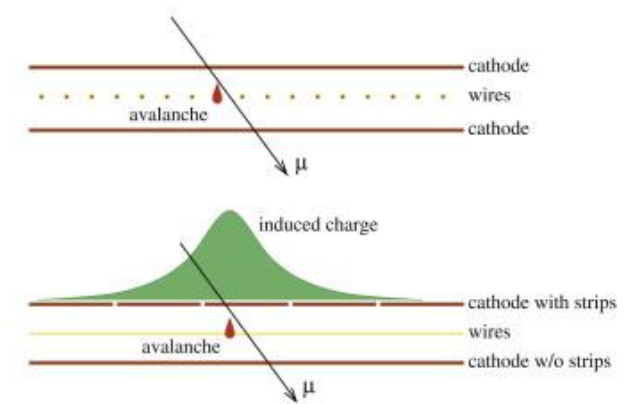
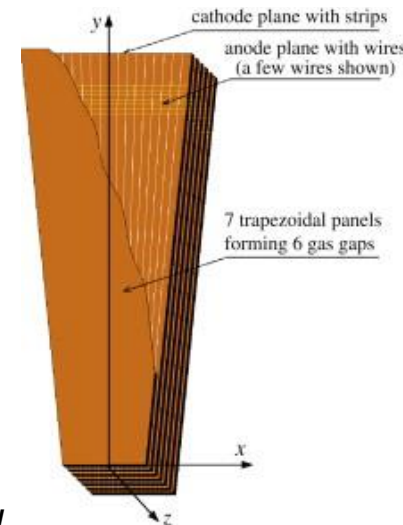
- Upgrade muon system in end caps for HL-LHC: $L=5 \times 10^{34} \text{ cm}^{-2}\text{s}^{-1}$
- CSC for **precise muon tracking and triggering**
- CMS: all endcap muon precision chambers are CSC
- ATLAS: CSC in low-angle region, Monitored DT (MDT) else
- HL-upgrades: readout with high speed optical links, trigger

Specifications:

CSC size:	3.3 x 1.5 / 0.8 m² (trapezoidal)
Number of layers	6 layers per chamber
Anode wire:	50µm W/Au-plated
Anode-cathode gap:	4.75 mm
Wire spacing:	3.12 mm
Number wire groups:	210'816, 5 to 16 wires per group
Cathode strip width:	8-16 mm (trapez.)
Number cathode strips:	266'112
Gas:	Ar(40%)+CO2(50%)+CF4(10%)
Maximum drift time:	60ns



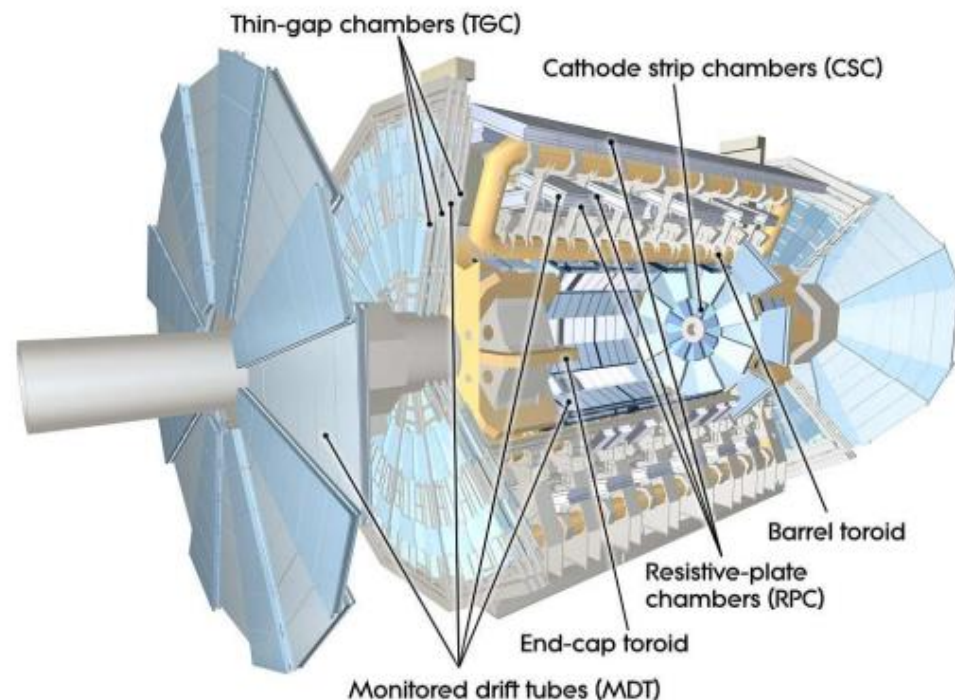
CSC with upgraded readout



4.3 Thin Gap Chamber

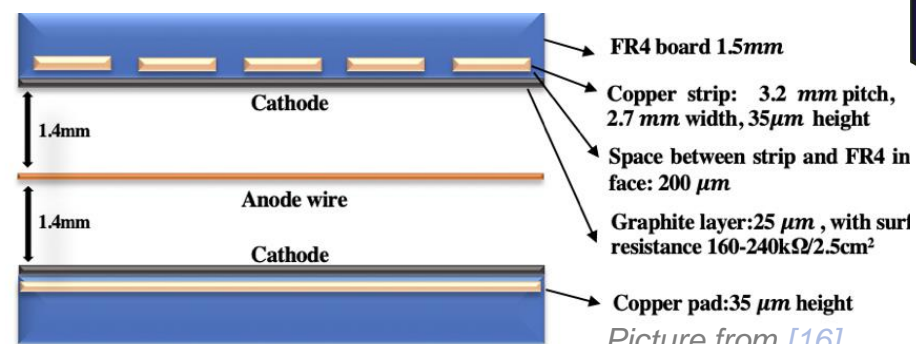
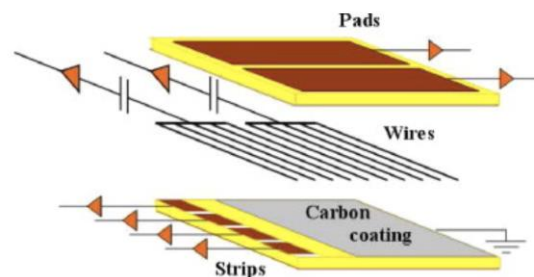
ATLAS NSW Upgrade for HL-LHC

- **Thin-Gap-Chamber (TGC) has smallest wire to cathode gap** [\[15,16\]](#)
- **sTGC with improved smaller cathode strip width**
 - upgrade the ATLAS muon endcap
 - new Small Wheel upgrade: fast trigger (<25 ns) and high precision tracking
 - 1mrad angular online resolution reduces fake muon trigger, 100µm spatial resolution (offline)
- small gap issue: **gain uniformity, high chamber flatness required**

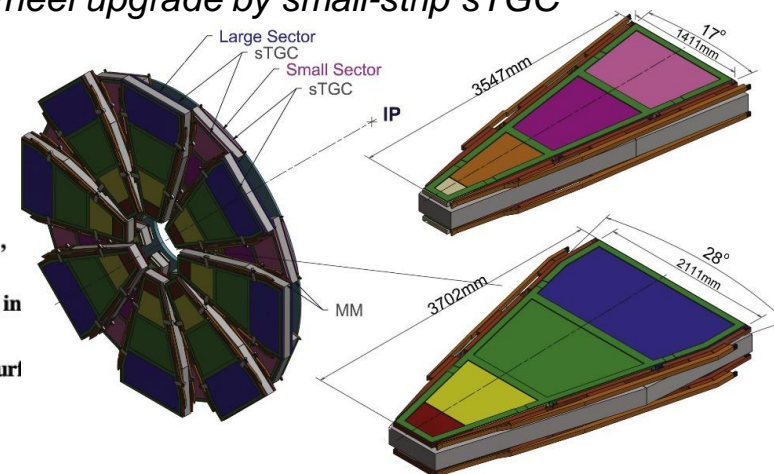


Specifications:

sTGC trapez. size:	3.7 x 2.1 / 0.5 m ²
HV:	2.8 kV
Gas mixture:	CO ₂ (55%)+n-Pentane
Wire pitch:	1.8 mm
Wire to cathode gap:	1.4 mm
Wire, diameter:	50 µm W(-Au)



New Small Wheel upgrade by small-strip sTGC

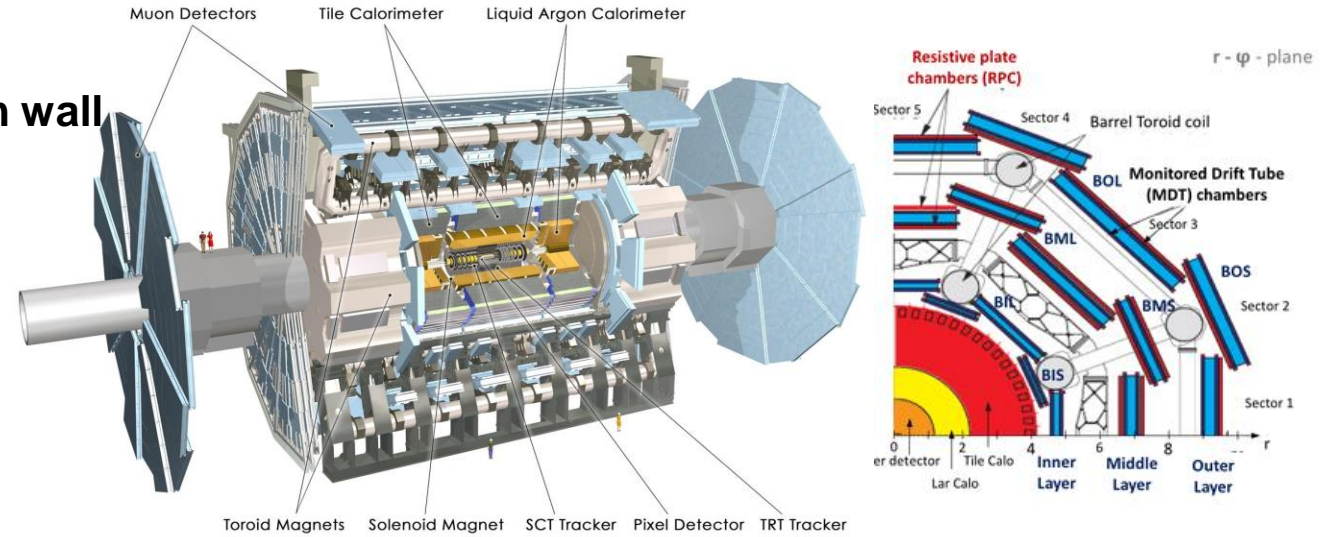


Picture from [\[16\]](#).

4.4 ATLAS-MDT/sMDT

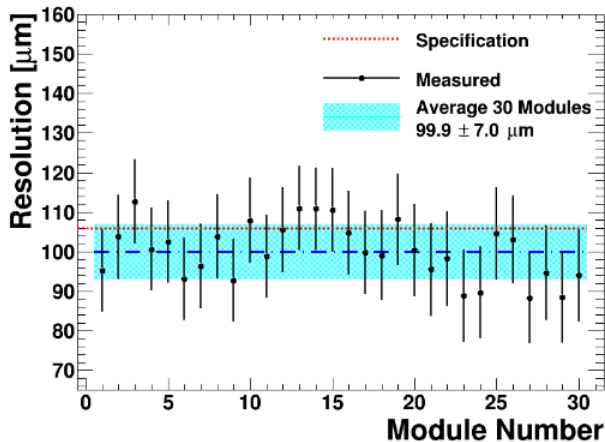
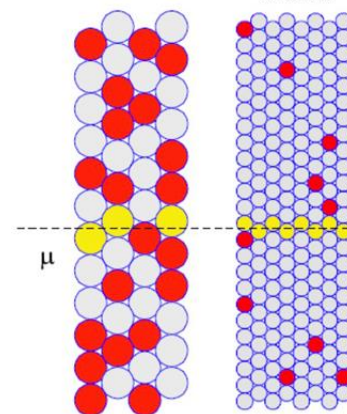
<http://dx.doi.org/10.1016/j.nima.2016.05.090>

- **Large-area and cost-efficient Muon Tracker**
- **Industrial aluminium tubes, 30/15mm diameter, 0.4mm wall**
- **Very high position accuracy**
 - Sense wire < 10 μm (rms)
 - Single hit spatial resolution $\sim 100 \mu\text{m}$
- **Upgrades for HL-LHC: new sMDT-RPC chambers**
 - 46080 new sMDT with 15mm diameter (MDT with $\varnothing=30\text{mm}$)
 - No ageing up to 9 C/cm tested ($\sim 15\text{x}$ MDT@LHC requirement)
 - Custom-designed ASD-ASIC (BLR, ADC added for charge integr.)
- **Perspective: further developments for FCC-ee/hh**



MDT
30 mm \varnothing

sMDT
15 mm \varnothing

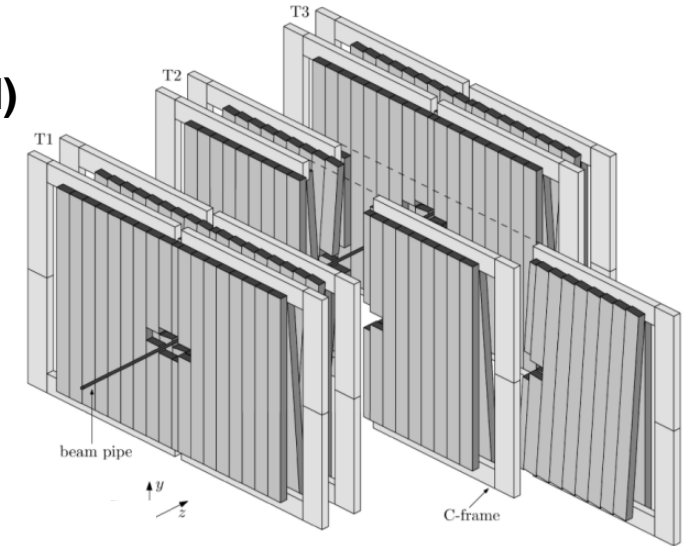
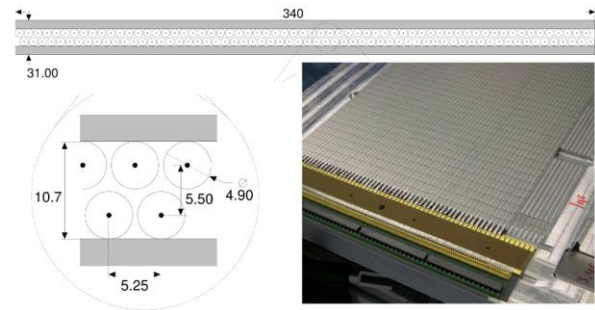


Parameter	Value	
Diameter	15 mm	OD
Wall	0.4 mm	Aluminium
Length	1.62 m	
Wire diameter	50 μm	W/Re
Gas	93/7	Ar/CO ₂
Gas pressure	3 bar	
Number tubes	46080	
Spat. resolution	$\sim 100 \mu\text{m}$	(σ)

4.5 LHCb Outer Tracker

<https://doi.org/10.1088/1748-0221/12/11/P11016>

- **Task: reconstruction of charged-particle trajectory and momentum (dipole B-field)**
- **53760 straws**, $\varnothing_{ID}=4.9\text{mm}$, 2.4m length
 - 25 μm diameter gold plated tungsten sense wire
 - 2 strips of Kapton-XC (40 μm + 25 μm), outer w/ 12.5 μm Al
 - $X = 0.1\% X_0/\text{layer}$
 - Ar/CO₂/O₂ (70/28.5/1.5), gas gain: 5.5×10^4
- **3 stations of 5x6m²**, 4x double-layers (x,u,v,x) per station
 - 128 straws glued to sandwich panels (Rohacell + 400 μm CF)
 - 168 long modules (4.85 x 0.34m²)
 - 96 short, inner modules (2.42 x 0.34m²)
- **Ageing effect seen after R&D phase, systematic study**
 - Source: plastifier changed in glue type, deposits by outgassing
 - Curing recipe developed (heating, 1.5% O₂, burn-off deposits)
- Operation ended 2018, status: no gain loss
 - 0.4 C/cm accumulated, 168 kHz/cm² max. flux



Parameter	Value	
Diameter	4.9 mm	ID
Wall	65/12 μm	Kapton-XC/ Al
Length	2.4 m	
Wire diameter	25 μm	W / Au-plated
Gas	70/28.5/1.5	Ar/CO ₂ /O ₂
Gas pressure	1.6 mbar	Overpressure
Number tubes	53760	
Spat. resolution	$\sim 200 \mu\text{m}$	(σ)



– **Sustainability: detector re-use and resource utilization, HEP → Hadron physics at FAIR**

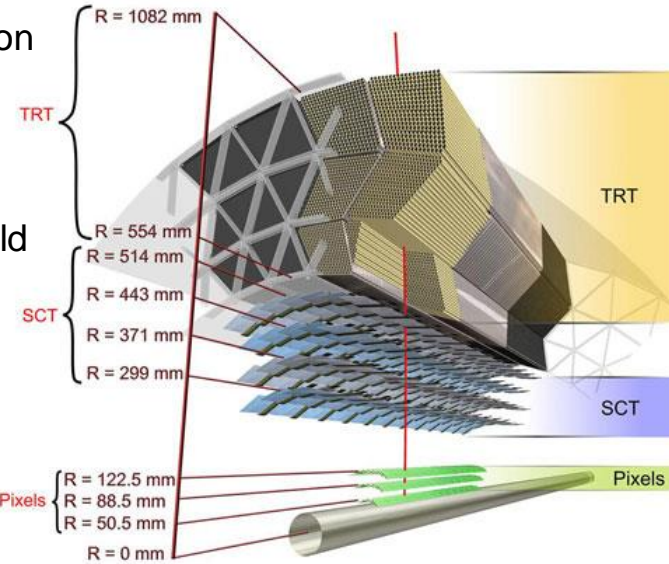
4.6 ATLAS – TR Tracker

• Tasks: electron identification and charged particle tracking

- TR photon (~10-30keV) detection for electron/pion separation
- Two-threshold ASDBLR (~ 300 eV/ 6 keV)
- Polypropylene radiator (fibers, foils)
- Hadron identification for low momenta by time-over-threshold
- 2T solenoid B-field

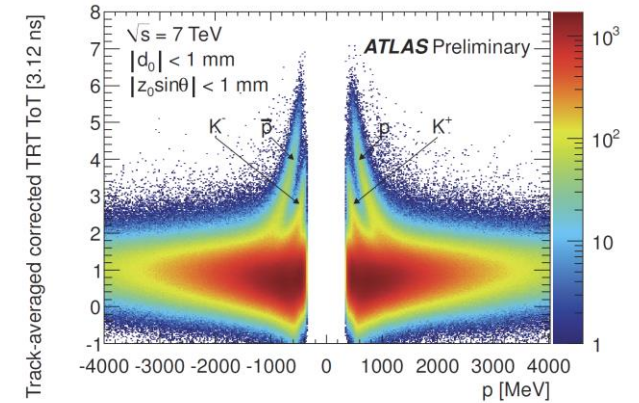
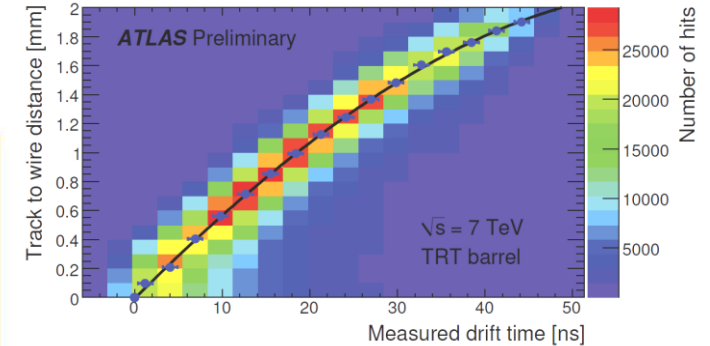
• Extreme conditions

- Charged particle flux up to $5 \times 10^5 \text{ cm}^{-2}\text{s}^{-1}$
- Photon flux up to $10^7 \text{ cm}^{-2}\text{s}^{-1}$
- Counting rate per straw 20 MHz
- Power dissipation by ionizing particles: 5 kW
- Charge collection up to 10 C/cm for 10y LHC operation
 - Extensive ageing studies (silicone, CF4, H2O, O2, ..)
- CF reinforced straw walls (4x strings)



Parameter	Value	
Diameter	4 mm	
Wall	70 μm	Kapton/Al-Kapton-XC
Length	1.44 m	Barrel part
Wire diameter	31 μm	Tungsten/ Au-plated
Gas	70/ 27/ 3	Xe/ CO2/ O2
Gas pressure	3 bar	
Number tubes	~ 300,000	
Spat. resolution	~ 130 μm (σ)	
Time resolution	~ 1 ns	

doi: 10.1016/j.phpro.2012.02.396



Carbon-doped Kapton tube wall with 4x CFiber reinforcement

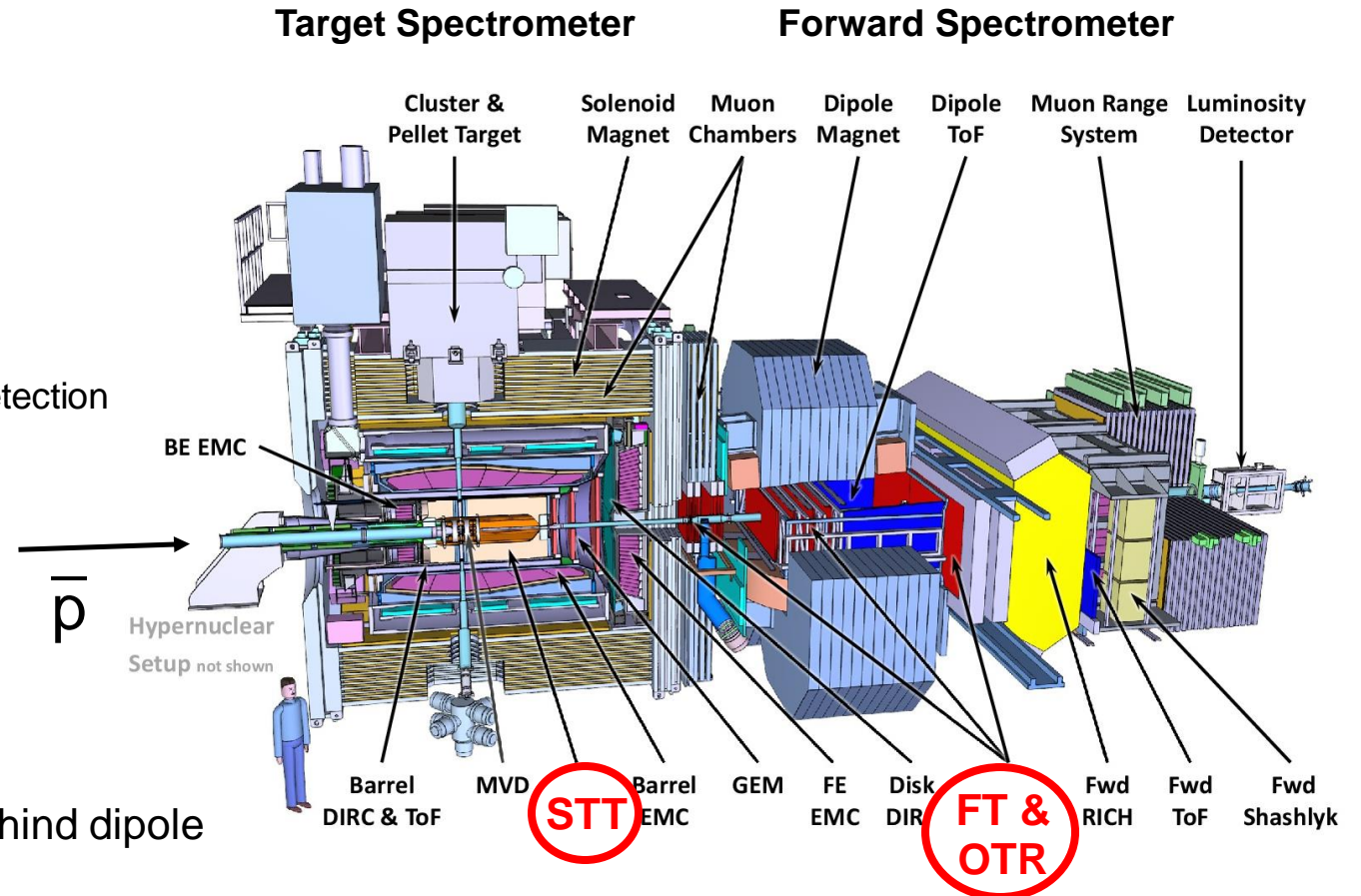


4.7 PANDA Straw Tubes

PANDA at FAIR with anti-proton beam (1.5-15 GeV/c) on p(A) target

- $\sqrt{s} \approx 2.2 - 5.5 \text{ GeV}$, $L=2 \times 10^{32} \text{ cm}^{-2}\text{s}^{-1}$, beam $\Delta p/p = 10^{-4}$
 - $2 \times 10^7 \text{ s}^{-1}$ anti-p p interactions at full luminosity
 - **$\sim 4\pi$ coverage and detecting all particle species**
 - 2T solenoid (TS) and 2Tm dipole (FS)
 - Good charged particle tracking (mom. resol. $\sim 1\%$)
 - broad momentum range: $\sim 100 \text{ MeV/c}$ to 8 GeV/c
 - delayed vertices (up to $\sim O(10 \text{ cm})$)
 - Particle identification (γ , e, μ , π , K, p), calorimetry, muon detection
-
- **Straw tube detectors**
 - **STT:** Central tracker with PID around IP
 - **FT:** Four forward tracker stations
 - **OTR:** Two forward tracker stations (LHCb-OTR) behind dipole

PANDA: Anti-Proton Annihilation at Darmstadt

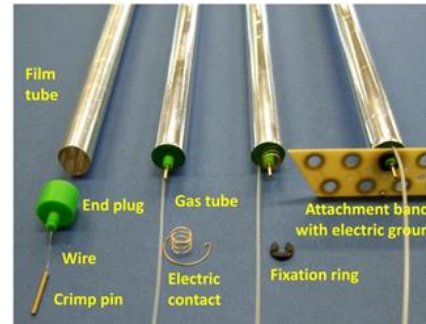


4.7 PANDA Straw Tube Tracker

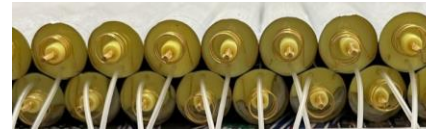
TDR: <https://arxiv.org/abs/1205.5441>

4D+PID central tracker in 2T solenoid B-field

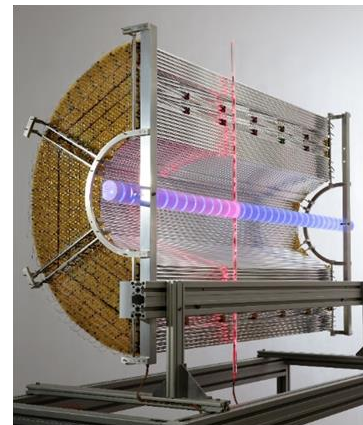
- 4224 straws in 19 axial + 8 stereo-layers ($\pm 3^\circ$)
- Close-packed, self-supporting layers by gas overpressure
- Low X/X_0 : $\sim 0.04\%$ per layer, $\sim 3.3\%$ in endcap region
- Drift time and time-over-threshold readout for PID
- Momentum resolution $\Delta p/p \sim 1-2\%$ (with MVD)
- Particle rates < 1 MHz per straw and < 10 kHz/cm²
- Continuous data stream readout (15 GB/s)
- Input for SW trigger by realtime event reconstruction



Straw components

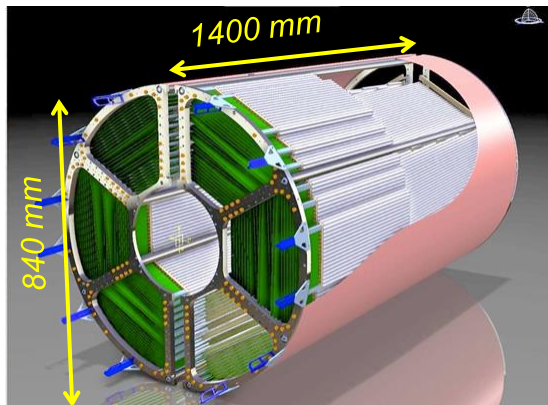


Close-packed layers ($40\mu\text{m}$ gaps)

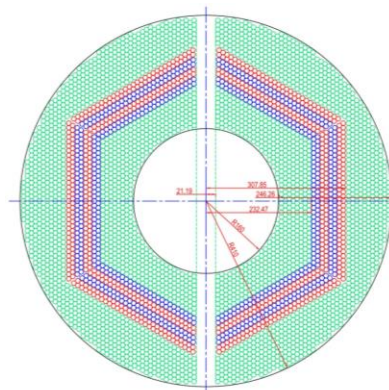


STT - prototype

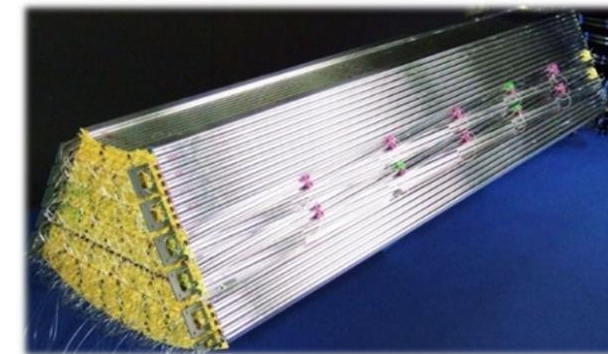
Parameter	Value	
Diameter	10 mm	ID
Wall	27 μm	Mylar-Al (1000 \AA)
Length	1.4 m	
Wire diameter	20 μm	W/Re(3), Au-plated
Gas	90/ 10	Ar/ CO ₂
Gas pressure	2 bar	1 bar overpressure
Material budget (X/X ₀)	0.04%	per layer
Number tubes	4224	
Number layers	19/ 8	Axial/ stereo-layers
Stereo angle	$\pm 3^\circ$	
Spatial resolution	150 μm	(σ , single hit)
Time resolution	~ 1 ns	
Total material budget (X/X ₀)	1.3%	incl. STT walls
Momentum resolution	1-2%	with MVD
Particle rates per straw	< 1 MHz	< 10 kHz/cm ²



PANDA-STT (3D-view)



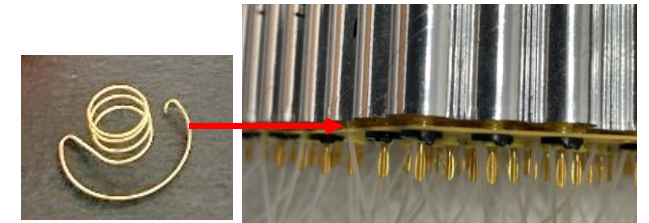
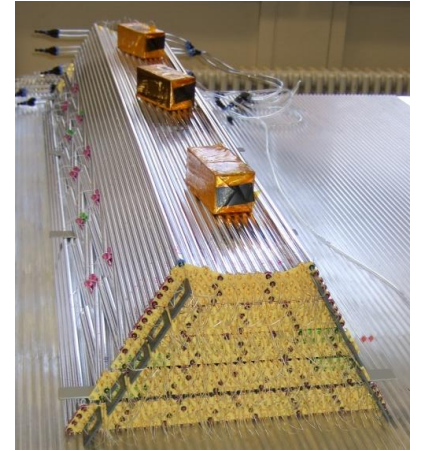
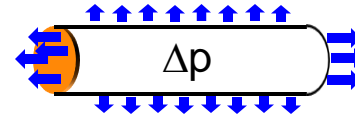
Straw layout (cross-view), stereo layers in red/blue.



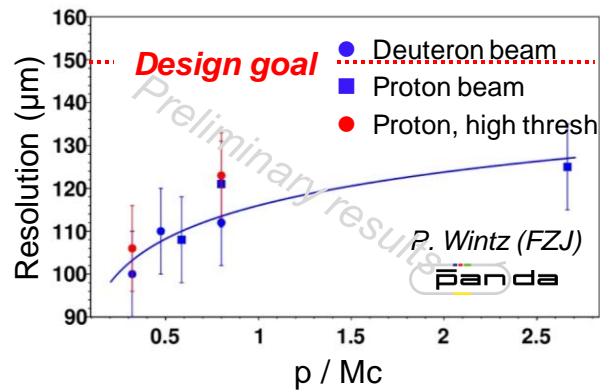
Hexagon sector prototype

4.7 PANDA Straw Tube Tracker

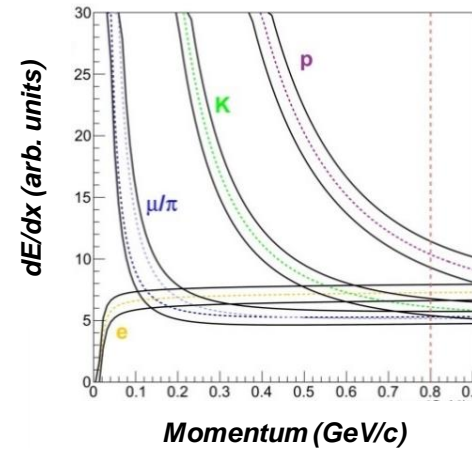
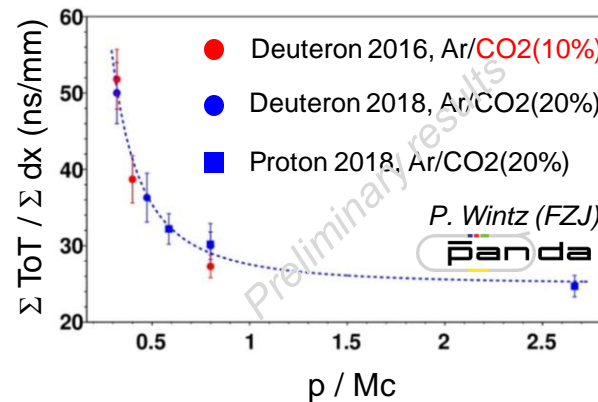
- **Aim: reduce detector material budget to minimum** for clean tracking in $\sim 0.1-10$ GeV/c momentum range
- **New technology invented: tube stretching by inner gas over-pressure** instead of by frame structure
 - homogenous (L, \varnothing) and strong tube stretching of $\Sigma F=32$ kN/STT ($\Delta p=1$ bar, $\varnothing=10$ mm tube)
 - spring-loaded suspension to allow elongation by rising over-pressure
- **Detector in construction**
 - development of application-specific readout ASIC (time, time-over-threshold readout)
 - prototype in-beam tests to verify design and measurement resolution goals



3x 3kg Pb bricks on top of hexagon modules (top). Spring-loaded suspension and electric ground contact of straw film tube.



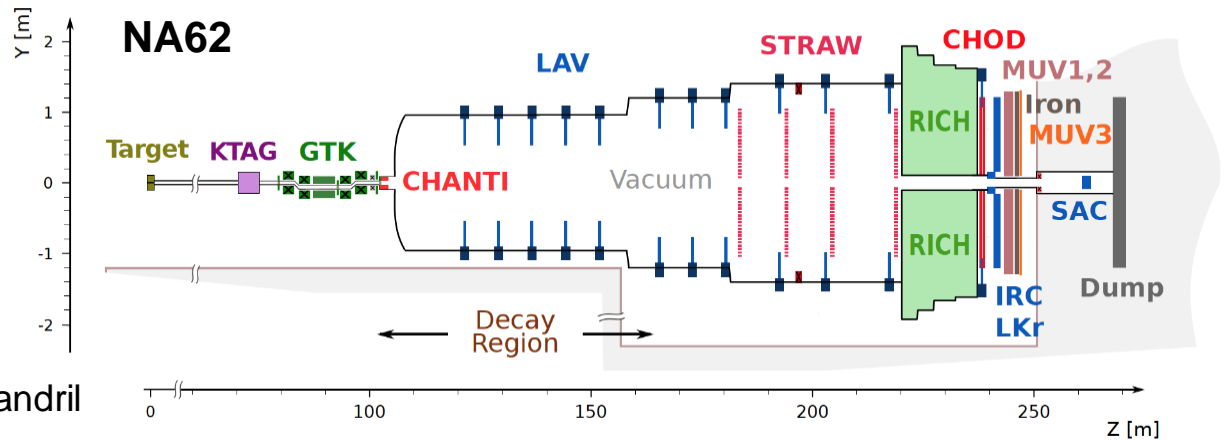
STT prototype measurements at COSY, (proton and deuteron beams)



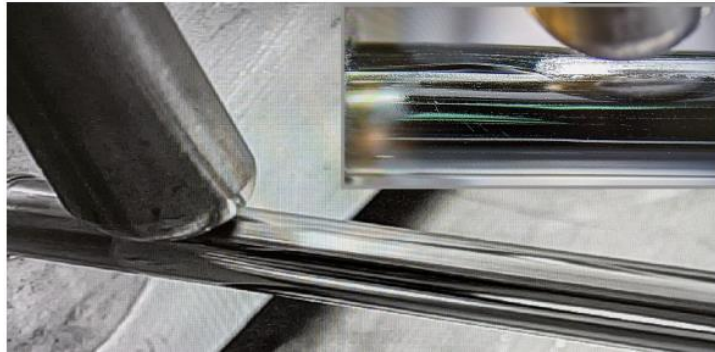
dE/dx simulation for STT

4.8 NA62 at SPS

- NA62 experiment to probe SM with **rare kaon decays**
- 1st large experiment with **straw tracker in vacuum**
- **Invented new specific straw tube winding technology**
 - ultra-sonic welding of PET film tube strip
 - longitudinal welding seam
 - conventional method: gluing two helically wound strips around mandril



NA62 Straw Station



Longitudinal welding of film tube (T. Enik, Straw Tracker 2024 workshop).

Parameter	NA62	(HIKE)
Straw diameter	9.82 mm	4.82 mm
Straw length	2.1 m	2.1 m
Straw wall (Mylar-Cu/Au)	36 μm	12 (19) μm
Wire diameter	30 μ m	20 (30) μ m
Gas	Ar/CO ₂ (30%)	Ar/CO ₂ (30%)
Gas pressure (abs.)	1 bar	1 bar
Number tubes	1792	5200
Planes per view	4	8
Total material budget (X/X ₀)	1.7%	1.0%
Maximum drift time	150ns	80ns
Trailing time resolution	30ns	6ns

<https://arxiv.org/abs/2311.08231>

<https://iopscience.iop.org/article/10.1088/1742-6596/2446/1/012036>

4.9 SAND for DUNE at FNAL

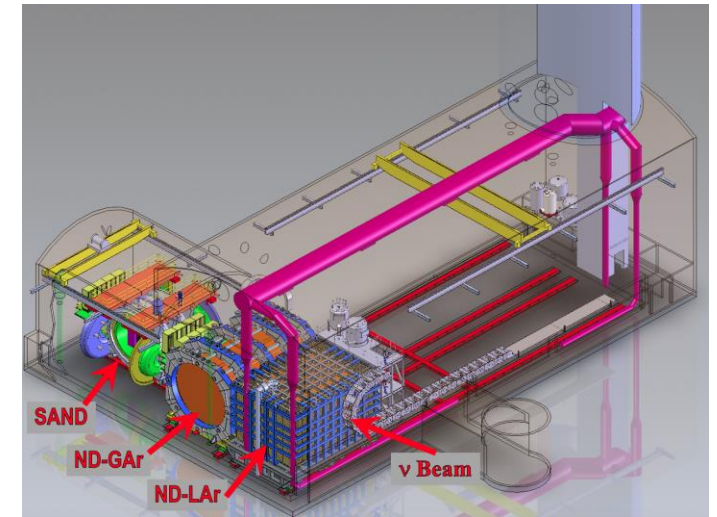
DUNE: Deep Underground Neutrino Experiment

<http://dx.doi.org/10.1393/ncc/i2023-23101-3>

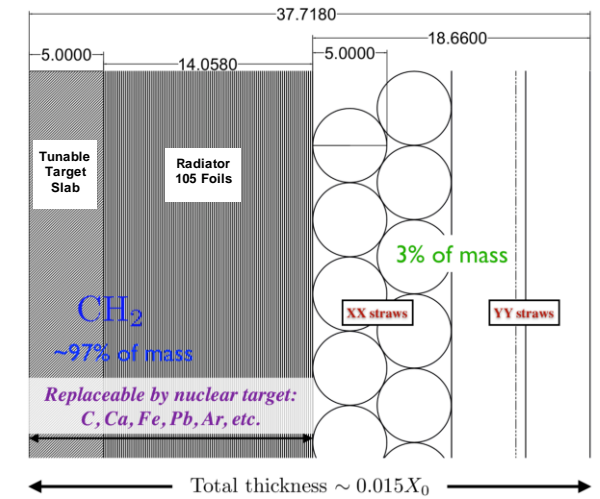
- **SAND: System for on-Axis Neutrino Detection** with novel detector concept
 - Separation of high purity targets (97% X0) from straw system (3% X0)
 - Target-tracker modules with total mass of ~5t, each module with
 - Tuneable neutrino passive target layers
 - Thin radiator polypropylene foils for e/π separation (transition radiation)
 - Four planes of straw tubes arranged as XXYY layers
 - CH₂ target modules (78) and carbon target modules (7)
 - Tracking modules with no target layers, PID by dE/dx, ..
 - Thin targets replaceable during data taking: C, Ca, Ar, Fe, Pb, ..
- **“Solid hydrogen target”** detector concept
 - Subtraction of measurements on pure C targets from on CH₂ target
 - Constrain nuclear effects and reduce systematic uncertainties
 - Provides ν/anti-ν - H high statistic, clean interaction sample



Photo from R. Petti, (STT for SAND)



Parameter	Value
Straw outer diameter	5 mm
Straw length (max.)	3.8 m
Straw length (avg.)	3.1 m
Straw wall (Mylar-Cu/Au)	15 μm
Gas	Xe/CO ₂ (30%)
Gas pressure (abs.)	1.9 bar
Number tubes	231,834
Number straw planes	368
Modules	92
Modules with CH ₂ target	78
Modules with graphite target	7

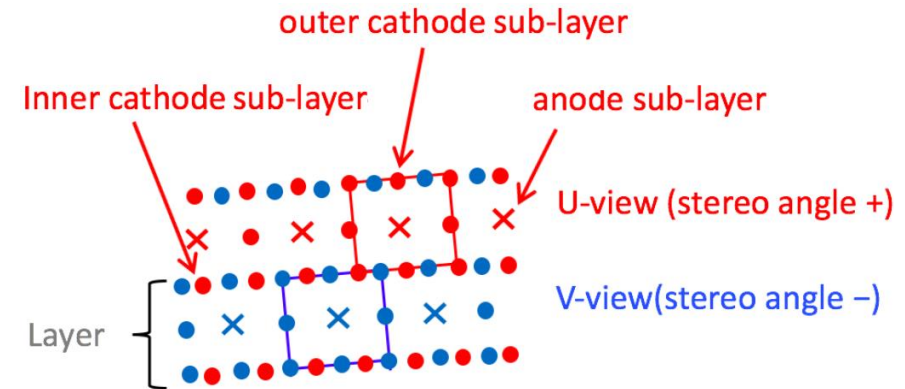


Layout of one CH₂ STT module

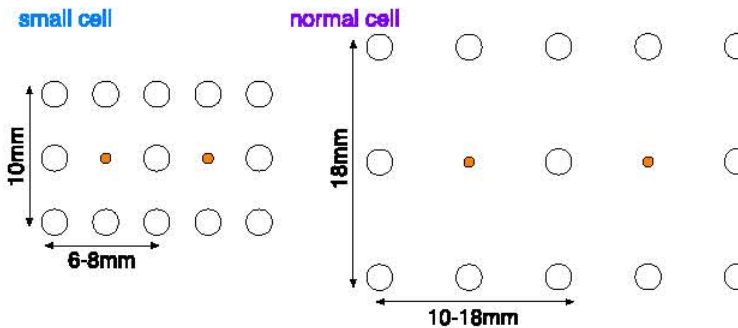
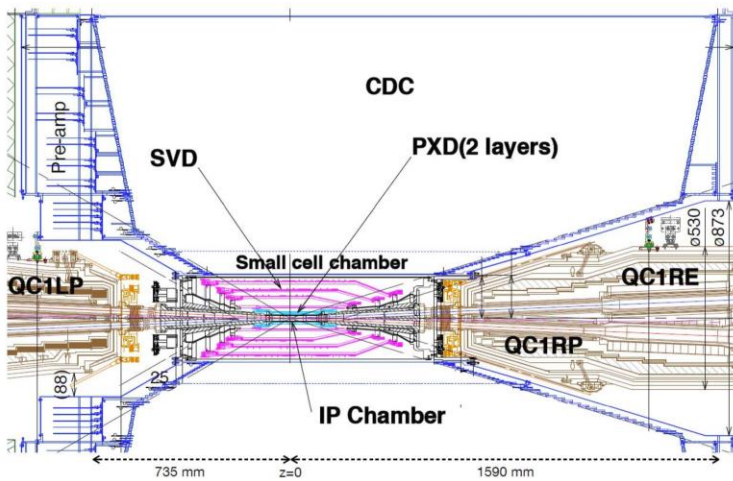
Interesting for future neutrino scattering and also next-generation, long-baseline neutrino oscillation experiments

4.10 Drift Chambers

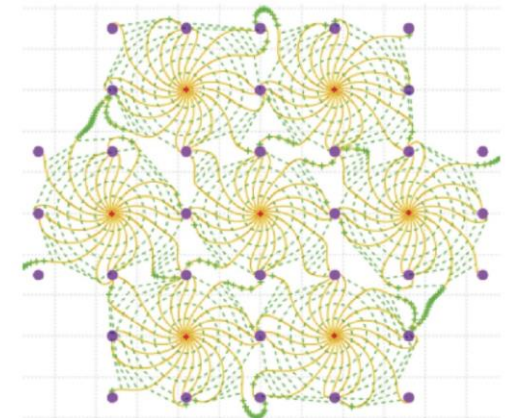
- **Feature: highest transv. momentum resolution tracking in solenoid B-field**
 - Large gas volume and long lever arm ($L \sim 1\text{m}$)
 - High transparency ($X/X_0 \sim 10^{-3}$) for low MS, favours He-based gas
 - **Helium requires high gas gain $\sim 5 \times 10^5$ (8 I.P./cm, ntp)**
- Small drift cells for short drift times (few 100ns), cathode wires surround anode
- Stereo drift cells for 3D-tracking, full stereo layout possible (in MEG-II DCH)
- dE/dx or ion cluster counting (dN/dx) for PID



Full stereo drift cell layout with high field homogeneity in MEG-II drift chamber [11].



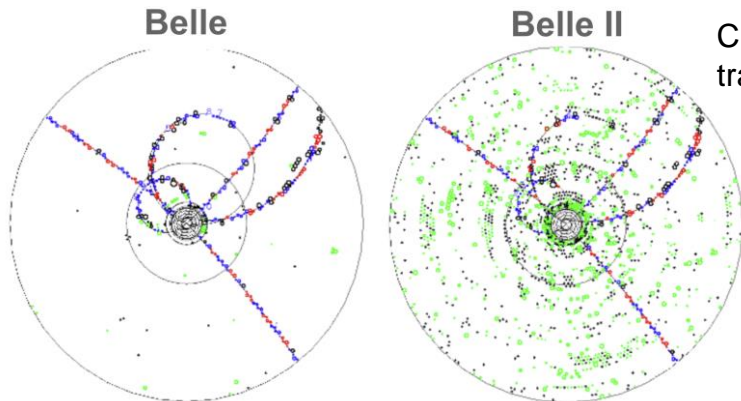
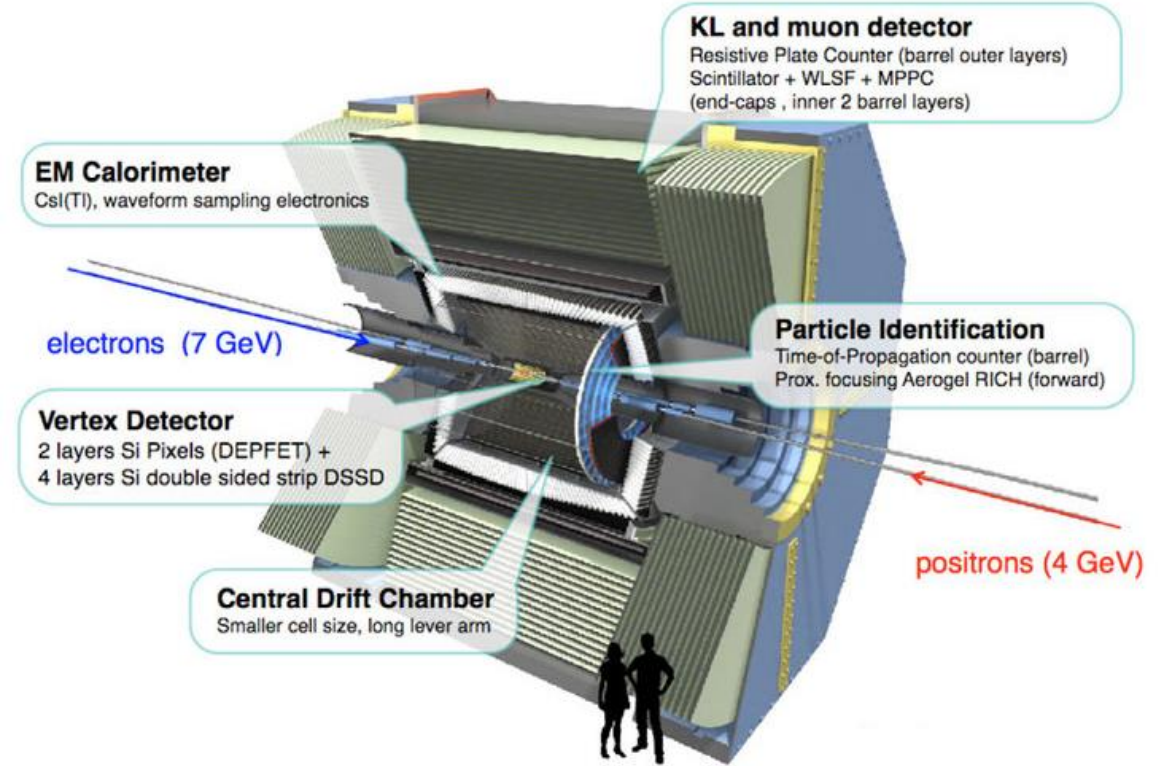
Belle drift chamber CDC (left). Smaller cells in inner region [10].



Electron drift lines for drift cells (Garfield simulation).

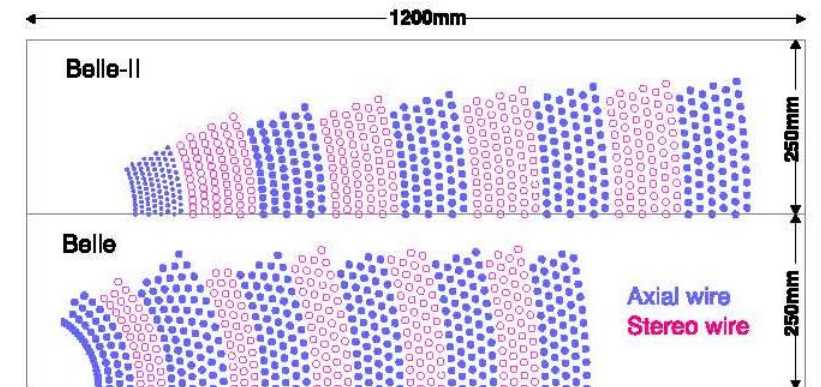
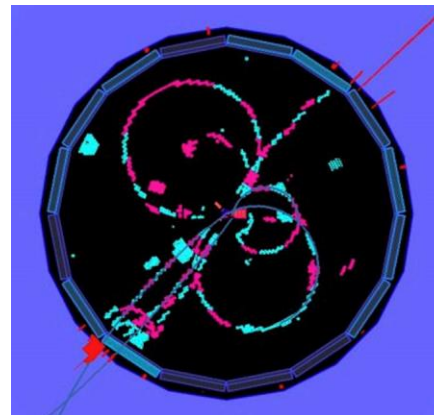
4.10 Drift Chambers

- Example: **Belle II CDC** at SuperKEKB (e^-e^+ collider, $\sqrt{s} \approx 10.6$ GeV)
- **Drift chamber at “extreme“ luminosity $L = 8 \times 10^{35} \text{ cm}^{-2} \text{ s}^{-1}$ [11]**
 - CDC in 1.5 T solenoid B-field
 - **R = 160 - 1130 mm, 2300 mm length**
 - **14k anode wires (30 μm W(Au), 129 μm Al cathode wires)**
 - **56 axial and stereo layers**
 - Drift gas He(50%) + C₂H₆
 - **$\sigma(\text{pt}) / \text{pt} \sim 0.1 \%$**
 - High occupancy: 11 tracks with ~ 100 hits, $\sim 10^4$ background hits
 - Particle momentum up to ~ 7 GeV/c, π/K separation ($\sim 90\%$)



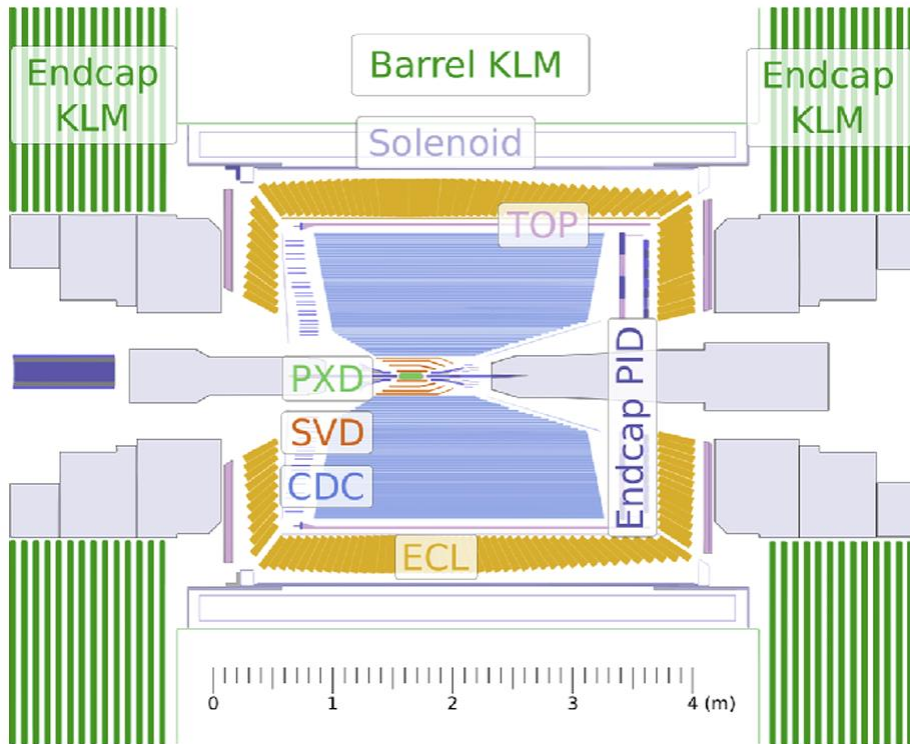
Challenge: low momentum tracks \rightarrow MS, curling tracks

First e^+e^- event in Belle II [11].

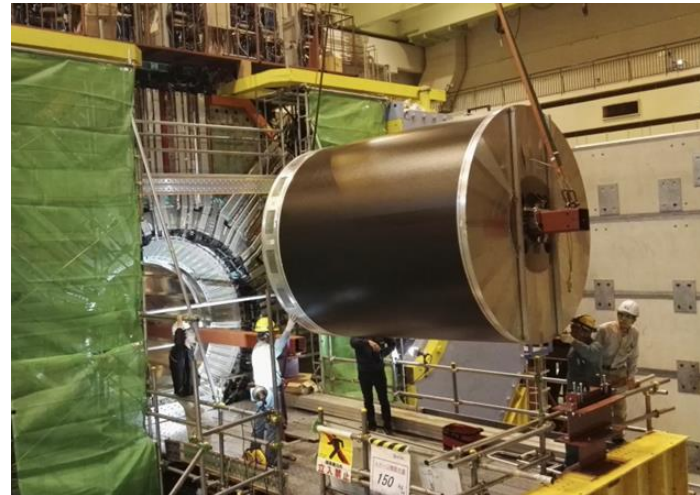


4.10 Belle II Central Drift Chamber

- Installation of CDC drift chamber in Belle II



Belle II layout of detectors.



CDC installation in Belle II.

CDC wire assembly.



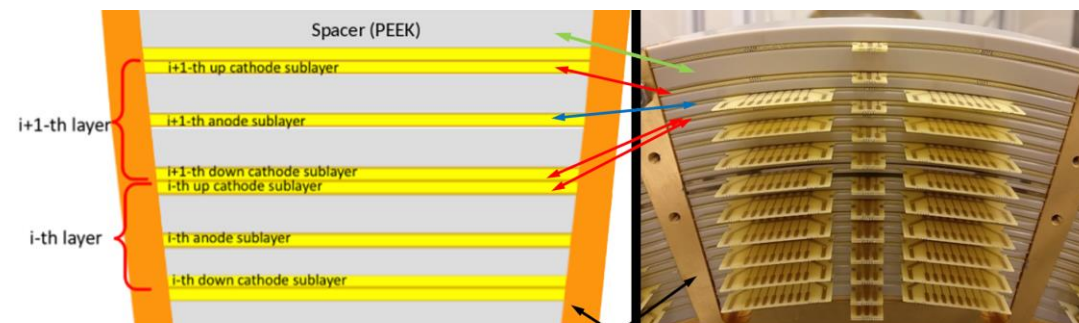
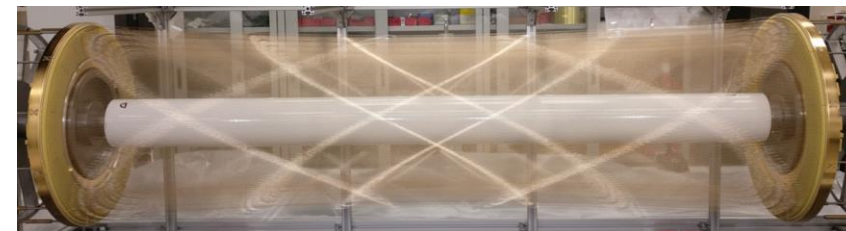
4.11 Drift Chamber

IDEA at FCC-ee

IDEA: full stereo, high resolution, ultra-light drift chamber [\[12\]](#), [\[13\]](#)

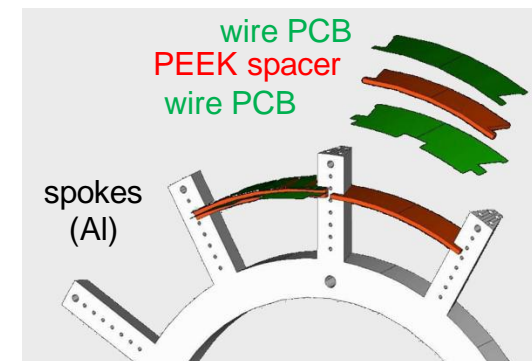
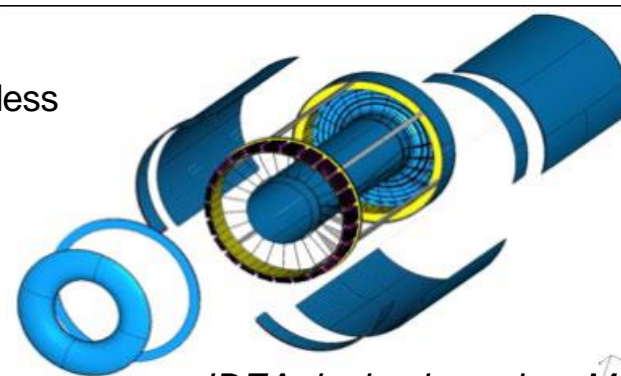
- 4000 mm length, 350-2000 mm radius in $\sim 2\text{T}$ solenoid B-field
- 14 SL \times 8 layers, 24 φ -sectors
- 56k sense wires, 20 μm diameter W(-Au)
- $\sim 290\text{k}$ field and guard wires, 40/50 μm diameter Al(-Ag)
- He(90%) + i-C₄H₁₀
- X/X₀ $\sim 0.1\%$ (end plate incl. FEE with X/X₀ \sim few %)
- Spatial resolution: $\sigma \sim 100\mu\text{m}$, mom. resolution: $\sigma(\text{pt})/\text{pt} < 0.3\%$

MEG-II drift chamber ($\mu \rightarrow e\gamma$ at PSI [\[11\]](#)).



Mechanics design

- construction featuring high granularity and high transparency
- novel wiring method (MEG-II wiring robot technique), feedthrough-less
- wire support mech. structure separated from gas volume envelop



IDEA design based on MEG-II

5. Summary

- Detector system technologies and properties

- Cathode-Strip-Chamber
- Thin-Gap-Chamber
- Drift Tubes
- Straw Tracker
- Vacuum Straw Tracker
- TR Straw Tracker
- Drift Chamber
- Multi-Wire-Proportional-Chamber

large area, low costs, robust, fast timing

large area, low costs, robust, high spatial resolution

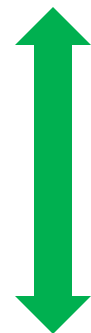
robust electrostatics, high resolution and fast timing, broad range of applications and detector geometries, “transparent” film tubes with robust in-vacuum operation, mixed with radiators for TR detection

large gas volume and lever arm, low MS for mom. resolution on ‰ level, cluster counting for PID

large area, transition radiation tracker

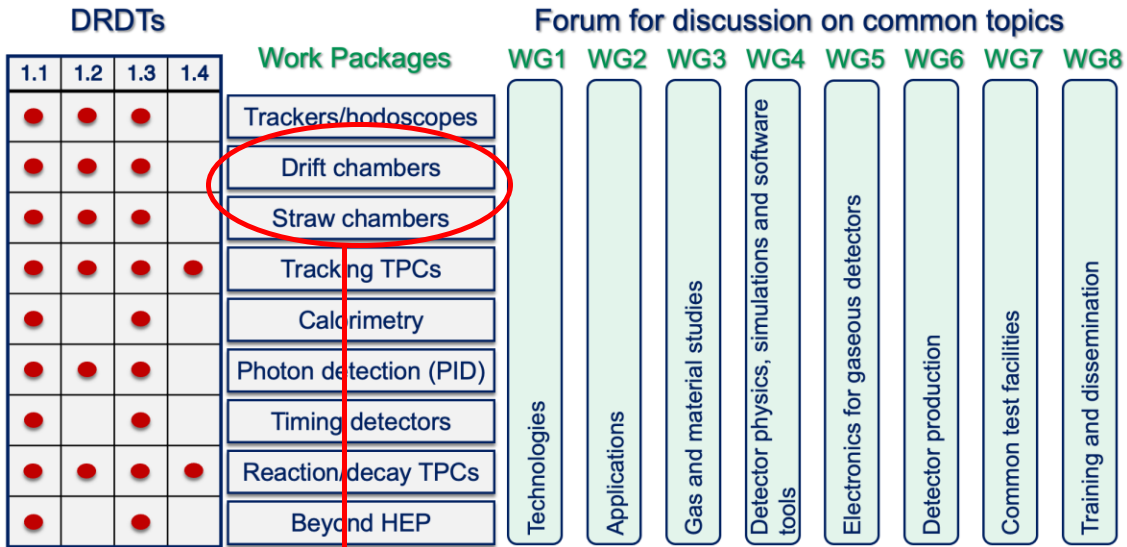
- Experiments with wire-based detector systems ranging from

- HEP
- Hadron physics
- Dark sector
- Rare decay experiments
- Neutrino physics



very broad application range and many future perspectives

6. Research Projects in DRD1

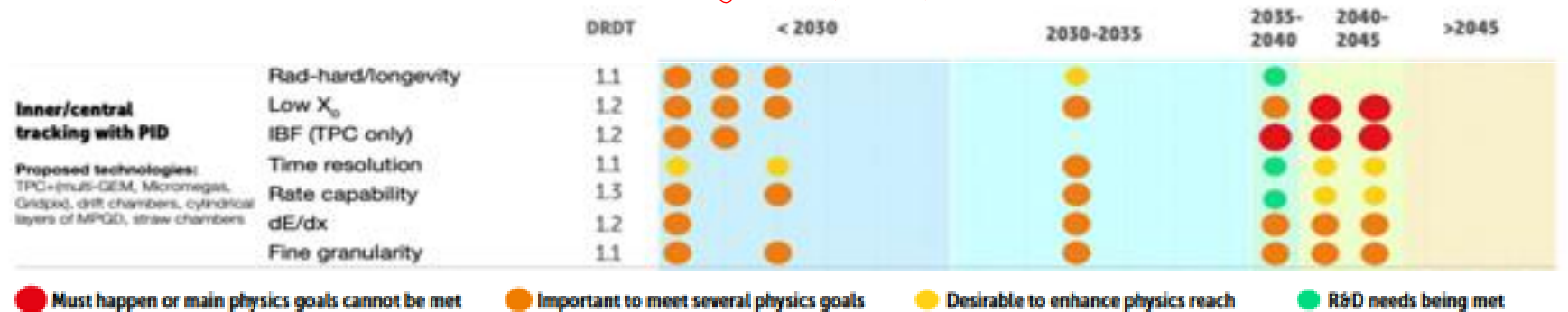
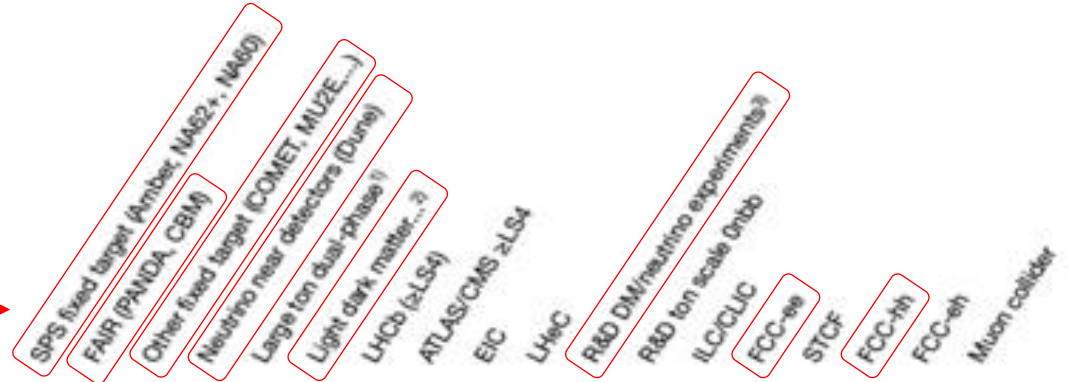


relevant for future experiments ..

ECFA

European Committee for Future Accelerators

- Experiments and detector R&D roadmap
- Two R&D work-packages in DRD1
 - Drift chambers
 - Straw chambers



Sketch from ECFA roadmap document and DRDT themes

***Thank you very much
for
your attention!***

References and Acknowledgement

- [10] I. Adachi et al., NIM A 907 (2018) 46–59; P. Rados Belle II Tracking Group, CHEP 2019
- [11] Eur. Phys. J. C (2018) 78:380 - <https://doi.org/10.1140/epjc/s10052-018-5845-6>; G. Tassielli (INFN Lecce), arXiv:2006.02378v2
- [12] <https://doi.org/10.1140/epjst/e2019-900045-4>, Eur. Phys. J. C (2018) 78:380
- [13] Eur. Phys. J. Special Topics 228, 261-623 (2019) - <https://doi.org/10.1140/epjst/e2019-900045-4>
- [14] N. Manganelli 2020 *JINST* **15** C03047 - <https://doi.org/10.1088/1748-0221/15/03/C03047>; <https://doi.org/10.1051/epjconf/201921402014>
- [15] D. Pudzha 2020 *JINST* **15** C09064, <https://doi.org/10.1016/j.nima.2015.11.095>
- [16] <https://doi.org/10.1088/1748-0221/15/09/C09021>

Useful literature (selection)

- W. Blum, W. Riegler, and L. Rolandi, Particle Detection with Drift Chambers, Springer-Verlag, Berlin (2008).
- Christian W. Fabjan, Herwig Schopper (Editors), Particle Physics Reference Library
- [S.. Rev. Navas et al. \(Particle Data Group\), Phys D **110**, 030001 \(2024\)](#)
- PDG: The Review of Particle Physics - <http://pdg.lbl.gov/>